Karson, J.A., Cannat, M., Miller, D.J., and Elthon, D. (Eds.), 1997
Proceedings of the Ocean Drilling Program, Scientific Results, Vol. 153

22. FLUID EVOLUTION IN SLOW-SPREADING ENVIRONMENTS[1]

Deborah S. Kelley[2]

ABSTRACT

Variably altered and deformed gabbroic and intercalated trondhjemitic to dioritic rocks, recovered from Ocean Drilling Program (ODP) Sites 921 to 923 near the eastern intersection of the Kane Fracture Zone and the Mid-Atlantic Ridge (MARK), display a complex history of interaction with magmatic fluids, high-temperature hydration within localized plastic deformation zones, and brittle failure. Pegmatitic patches, oxide gabbros, and felsic veins, which occur throughout the core and that contain abundant apatite, zircon, oxide minerals, and coarse-grained amphibole, are thought to have crystallized under relatively high fO_2 from a hydrous magma. Analyses of primary fluid inclusions in magmatic apatite in these evolved rocks show that the earliest fluids to be exsolved from the melts involved CO_2-rich vapors, which with progressive fractionation evolved to more H_2O-rich compositions. These later fluids were most likely exsolved under immiscible conditions, resulting in the development of CO_2-H_2O-rich vapors and CO_2-H_2O-NaCl brines that were trapped during mineral growth, as well as during later high-temperature fracturing events. In trondhjemitic to dioritic veins that cut the plutonic sequence, subsequent cooling of the high-salinity, magmatic fluids during the final stages of crystallization, or direct exsolution of brines from the late-stage melts, resulted in formation of fluids with equivalent salinities of 38–59 wt% NaCl. With continued cooling, brittle fracturing at minimum temperatures of 275°–350°C allowed circulation of hydrothermal fluids with salinities that ranged from near seawater to six times that of seawater values (1–20 wt% NaCl equivalent).

A striking result of this study is the discovery of fluids rich in CH_4, H_2O, $\pm H_2$ along healed microfractures in the plutonic rocks that contain up to 11 mol% CH_4, which were entrapped at minimum temperatures of 270°–365°C. The high concentration of $CH_4 \pm H_2$ in these fluids most likely reflects high-temperature oxidation of iron within mafic minerals during seawater alteration of the plutonic rocks at low water-rock ratios, coupled with the release of H_2 during magnetite formation, and attendant CO_2 reduction. The discovery of CH_4-rich fluids in crustal Layer 3 rocks from both the MARK area and from ODP Hole 735B on the Southwest Indian Ridge suggests that oceanic crustal Layer 3 may represent a significant, presently unrecognized sink for carbon. Leaching during subsequent hydrothermal alteration may play an important role in the transfer of carbon from the lithosphere to the hydrosphere.

INTRODUCTION

Recent studies concerning the interaction between magmatic, hydrothermal, and tectonic processes at mid-ocean ridge spreading centers indicate that, perhaps more than any other factor, volatiles provide a common thread that link geodynamic, geologic, and geobiological processes acting in mid-ocean ridge environments. Volatile species such as CO_2 and H_2O govern the physical properties of melts and profoundly influence the eruptive and deformational behavior of magma chambers (Taylor and Green, 1987; Stolper and Holloway, 1988; Sparks et al., 1994). In turn, the degassing histories of magma chambers exert a dominant control on the absolute volatile concentration in any overlying hydrothermal system. Submarine eruptive events may result in the cataclysmic release of magmatic volatiles into the hydrosphere, as evidenced by the recent discovery of megaplumes that exhibit anomalous ^{3}He/heat ratios and transient heat fluxes that increase to at least 100 times those of active vent fields (Lupton et al., 1989; Baker et al., 1993; 1995; Embley et al., 1995; W.S.D. Wilcock, unpubl. data), and more steady state degassing of volatile species (e.g., He and CH_4) into the water-column provides a key tracer of hydrothermal sites on the seafloor (Lupton and Craig, 1981; Lupton, 1983; Jean-Baptiste et al., 1991; Charlou et al., 1992; Lilley et al., 1992; Baker et al., 1993). Volatiles also play a critical role in submarine microbial development. The close association of enhanced volatile flux (CO_2, H_2S, and He) and an associated massive efflux of microbial material from fractures in the seafloor during eruptive events on the East Pacific Rise and on the Juan de Fuca Ridge has led to the hypothesis that magmatic gases released during volcanic eruptions provide important nutrients necessary for sustaining both subsurface and surface microbial communities (Haymon et al., 1993; Demming and Baross, 1993; Delaney et al., 1994; Lilley, 1994; Baker et al., 1995). In addition, deep-seated circulation of supercritical CH_4- and CO_2-rich hydrothermal fluids through the crust may provide efficient alteration and scavenging of hydrothermal organic compounds that most likely contribute to this nutrient source (Simoneit, 1993). Although these and similar studies have dramatically increased our understanding of the nature of volatiles in the shallow component of submarine hydrothermal systems, direct knowledge of the nature and evolution of fluids in rocks formed 2–5 km below the seafloor is limited as a result of the difficulty in sampling deeper crustal levels and analytical limitations associated with measuring fluids entrapped within the recovered rocks.

In 1994, the Ocean Drilling Program (ODP) successfully drilled Sites 920–924 at the MARK area of the Mid-Atlantic Ridge (Fig. 1) to investigate the relationships between magmatic, tectonic, and hydrothermal processes acting during accretion of upper mantle and lower crustal rocks formed in a slow-spreading ridge environment (25 mm/yr). The ultramafic and gabbroic lithologies recovered from these sites record complex histories involving the integrated effects of polyphase deformational episodes, intrusion of gabbroic and felsic veins, and progressive strain localization and metamorphic recrystallization. In this study, analyses of fluids entrapped in plutonic rocks recovered from Sites 921 to 923 are used to provide new insight into the geochemical history and the distribution of volatiles in the near solidus to subsolidus environment and to assess their potential importance in geochemical processes acting in the lower crustal component of submarine hydrothermal systems.

[1]Karson, J.A., Cannat, M., Miller, D.J., and Elthon, D. (Eds.), 1997. *Proc. ODP, Sci. Results,* 153: College Station, TX (Ocean Drilling Program).

[2]School of Oceanography, University of Washington, Seattle, WA, 98195, U.S.A.
kelley@ocean.washington.edu

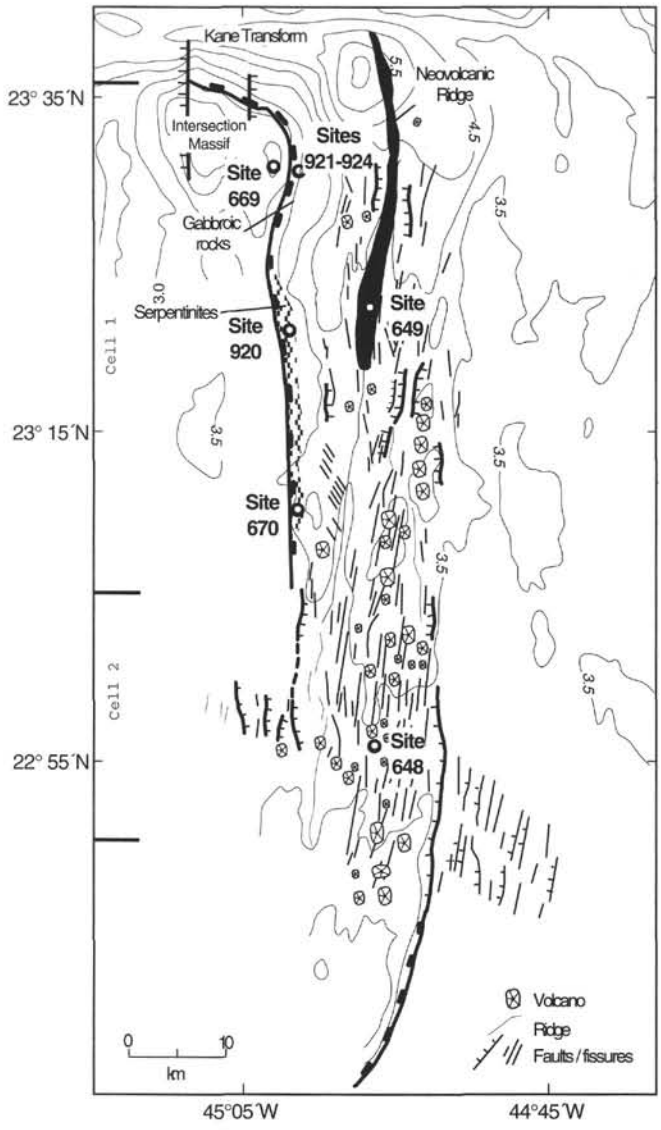

Figure. 1. Location of Sites 920–924 near the eastern intersection of the Mid-Atlantic Ridge and the Kane Fracture Zone (MARK). The interior corner high is dominated by gabbroic outcrops. Sites are shown as open circles. The zigzag line represents area of serpentinite outcrops identified from submersible studies and dredging (after Shipboard Scientific Party, 1995).

Fluid inclusion data presented in this paper build upon earlier studies of plutonic and extrusive samples from the MARK area (Gallinatti, 1984; Kelley and Delaney, 1987; Delaney et al., 1987; Kelley et al., 1993; Saccocia and Gillis, 1995). These data indicate that fluid inclusions trapped during mineral growth and during subsequent fracturing events are the product of multiple pulses of both magmatic- and seawater-derived hydrothermal fluids. Fluid inclusions in primary and alteration mineral phases record a complex history of volatile evolution that initially involved exsolution of magmatic CO_2-rich fluids and later penetration of hydrothermal seawater under greenschist facies metamorphic conditions. One of the latest hydrothermal events involved circulation of fluids with CH_4 concentrations approximately 11 times those of hydrothermal vent fluids and of basalt-hosted volcanic gases. In the following discussion, the spatial distribution and thermal-compositional character of fluids entrapped within the plutonic rocks from Sites 921 to 923 are described, their potential sources are considered, and a model for the evolution of these fluids at depth is presented.

Tectonic Setting and Geologic Overview of the MARK Area

The MARK area (Fig. 1) is one of the best characterized regions of the Mid-Atlantic Ridge. It offers an excellent opportunity to examine the interplay between magmatic, tectonic, and hydrothermal processes in the context of a slow-spreading environment. It has been the site of numerous geophysical (Cormier et al., 1984; Purdy and Detrick, 1986; Schulz et al., 1988), bathymetric (Detrick et al., 1984; Karson et al., 1987; Pockalny et al., 1988), and sidescan surveys (Kong et al., 1989; J.R. Delaney and J.A. Karson, unpubl. data) and has been extensively sampled by dredging (Karson and Dick, 1983), by submersible dives (Karson and Dick,1983; Mével et al., 1991; Gente et al., 1991), and by two ODP studies (Legs 109 and 153). Data collected during these programs have delineated at least two spreading cells in the MARK area: a northern cell (cell 1) extending from the northern nodal basin to ~23°18′N and a southern cell (cell 2) beginning south of 23°05′N (Fig. 1). A broad discordant zone, interpreted as a zero offset transform fault (Purdy and Detrick, 1986), separates these two cells (Fig. 1). The axial rift valley in the northern cell is characterized by a continuous median valley ridge, which narrows and deepens as the ridge-transform intersection is approached. This volcanic ridge is bounded to the north by the opposing transform valley wall and to the west by a nodal basin >6000 m deep. Westward of this basin, within a distance of 15 km, extreme uplift of the crustal/mantle section has produced a lithologically complex massif that shallows to 1400 m depth and exposes crust approximately 500,000 to 900,000 yr old (Shipboard Scientific Party, 1995). The walls of this massif are dissected by a series of steeply dipping (50°–70°), eastward-facing fault scarps, which subparallel the ridge axis and impart an overall stair-step morphology to the median valley walls (Karson and Dick, 1983; Mével et al., 1991). Photographic traverses and observations from the *Alvin* and *Nautile* show that the western wall is composed of a complex juxtaposition of lithologies, which include hydrothermally altered basaltic, upper and lower crustal plutonic rocks, as well as peridotites (Karson and Dick, 1983; Karson et al., 1987; Brown and Karson, 1988; Mével et al., 1991). The distribution of lithologic, alteration, and deformation types suggests that the intersection massif is composed of allochthonous blocks bounded by high-angle faults (Karson, 1990) and that the master or bounding fault(s) is/are either an undulating low-angle detachment surface or a series of subparallel faults. In contrast to the extreme relief observed at the western side of the ridge-transform intersection, the eastern valley walls exhibit more subdued topography and are characterized predominantly by basaltic outcrops and flows (Karson and Dick, 1983; Mével et al., 1991).

South of the ridge-transform intersection, near the discordant zone and at the edge of the northern cell, two serpentinite outcrops have been sampled by dredge (Gente et al., 1991), dive programs (Karson et al., 1987; Mével et al., 1991), and drilling at ODP Sites 670 and 920 during Legs 109 and 153. Serpentinized harzburgites and lherzolites recovered during these programs exhibit high-temperature, plastic deformation overprinted by serpentinization (et al., 1990; Mével et al., 1991; Shipboard Scientific Party, 1995). Emplacement of these mantle rocks is thought to result from lithospheric stretching associated with amagmatic extension.

Variably altered and deformed plutonic rocks collected from the MARK area during previous submersible and dredging programs range from olivine gabbro, to ferrogabbro, to plagiogranite (Gillis et al., 1993; Kelley et al., 1993). The plutonic rocks record a complicated alteration and deformational history, starting at temperatures in excess of 700°C (Kelley and Delaney, 1987; Gillis et al., 1993;

Kelley et al., 1993). In some of the metagabbroic rocks, this high-temperature deformation and recrystallization has been interpreted to represent ductile shear zones that may reflect initiation of faulting in the near axis environment (Karson and Dick, 1983; Gillis et al., 1993; Mével et al., 1991). The relative timing and penetrative depth of these extensional features is not clear, however. The shear zones allowed enhanced penetration of fluids, which locally resulted in pervasive high-temperature alteration at temperatures >500°C (Gillis et al., 1993; Kelley et al., 1993). The plutonic samples commonly have undergone brittle deformation in the form of microfractures to millimeter-wide fractures that are filled with lower amphibolite to greenschist facies mineral assemblages. The degree of alteration within individual samples may be quite heterogeneous; the most pervasive alteration is adjacent to fractures. Most samples are crosscut by narrow (<1 mm wide) stringers filled with acicular amphibole and/or chlorite, which may or may not be continuous across a sample. Quartz-cemented, sulfide-bearing breccias are interpreted to represent the 300°C upflow conduits of deep-seated paleohydrothermal systems (Delaney et al., 1987; Kelley et al., 1993). The breccias are thought to have formed within fault-bounded veins that were periodically reactivated and that involved fluids that intermittently achieved velocities >1 m/s (Delaney et al., 1987). Metabasalts collected from this area are variably altered under greenschist to zeolite facies metamorphic conditions. Low-temperature, vein-filling minerals and fluid inclusions indicate that cessation of seawater penetration occurred at temperatures of about 180°C (Kelley et al., 1993).

Sites 921–924

Drilling at Sites 921–924 successfully penetrated into tectonically exposed windows of deep to shallow crustal rocks that are thought to have formed beneath the median valley of the slow-spreading Mid-Atlantic Ridge 500,000–900,000 yr ago (Fig. 1). Intrusive relationships and the geochemical composition of these rocks indicate that the crust in this region was formed by a series of mafic intrusions that, similar to plutonic rocks from Hole 735B, commonly show evidence of syn- to post-magmatic high-temperature deformation.

Plutonic rocks recovered at Sites 921–924 exhibit a wide range in composition that includes variably altered and deformed olivine gabbro and troctolite (~65%)(Fig. 2A) with lesser amounts of gabbro and iron oxide gabbro (8%), intermixed gabbro and olivine gabbro (20%)(Fig. 2B), and minor diabase (~1%). Compositional layering and cryptic variation in these rocks is best preserved in core from Hole 923A, although layering patterns are partially preserved in core from the other sites as well (see Casey, this volume). Variation in grain size and degree of deformation is extremely heterogeneous on a centimeter to meter scale; pegmatitic pods and crystal plastic deformation are common. The pegmatitic patches contain abundant apatite, zircon, oxide minerals, and coarse-grained amphibole and are thought to have crystallized under relatively high fO_2 from a hydrous magma (Fig. 3). The pegmatitic patches may reflect equilibration of the evolved melts with volatile-rich fluids that percolated through the gabbroic sequence late in the magmatic history. Intense deformation is commonly associated with narrow zones of oxide gabbro in which stringers of iron titanium oxide form a wrapping foliation. Discrete and net veins of trondhjemitic to dioritic material represent the last phase of igneous activity (Fig. 4).

METAMORPHISM

The variably altered and deformed gabbroic and intercalated trondhjemitic to dioritic rocks display a rich history of interaction with magmatic fluids, high-temperature hydration within localized plastic deformation zones, and brittle failure that resulted in localized patches of pervasive alteration under greenschist metamorphic conditions. Magmatic and metamorphic processes exhibit a progressive evolution with the transitional merging of crystal fabrics that are strictly magmatic to those associated with lower temperature deformation. The crystal-plastic fabric observed in discrete and heterogeneously distributed shear zones throughout the cores is commonly associated with synkinematic hornblende and recrystallized olivine, plagioclase, and pyroxene, indicating that recrystallization and deformation occurred at temperatures of 700°–>900°C, under amphibolite to transitional granulite facies metamorphic conditions (Liou et al., 1974; Spear, 1981). The mylonitic to protomylonitic zones are characterized by anastomosing bands of fine- to very fine-grained neoblastic plagioclase, which commonly exhibits a well-developed mo-

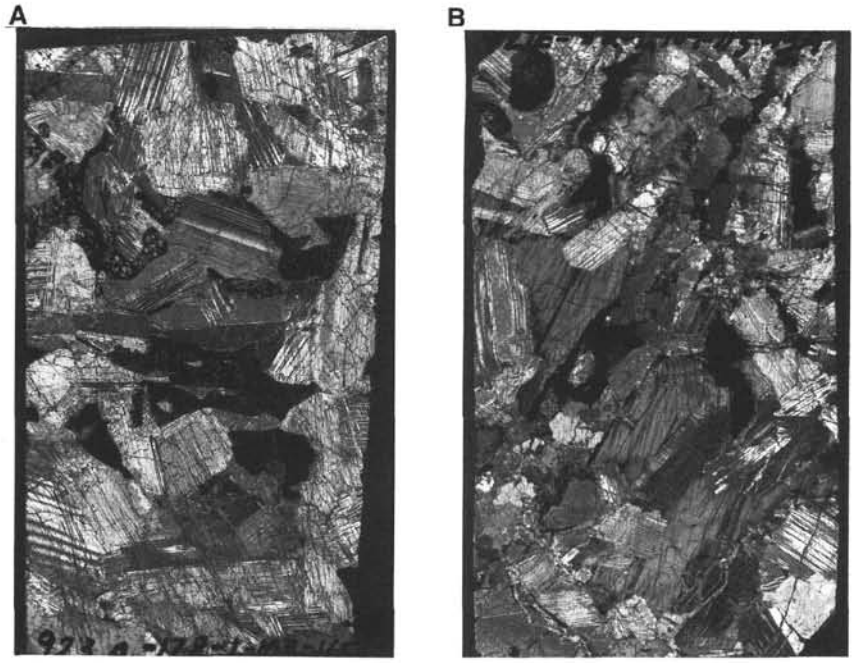

Figure. 2. Photomicrographs of **(A)** olivine gabbro. Dark, highly fractured grains are moderately altered olivine crystals (Sample 153-923A-12R-1, Piece 5B, 109–113 cm), and **(B)** mildly deformed gabbro cut by narrow felsic vein (Sample 153-921E-8R-1, Piece 13A, 109–113 cm). Sections are 4.5 cm in length.

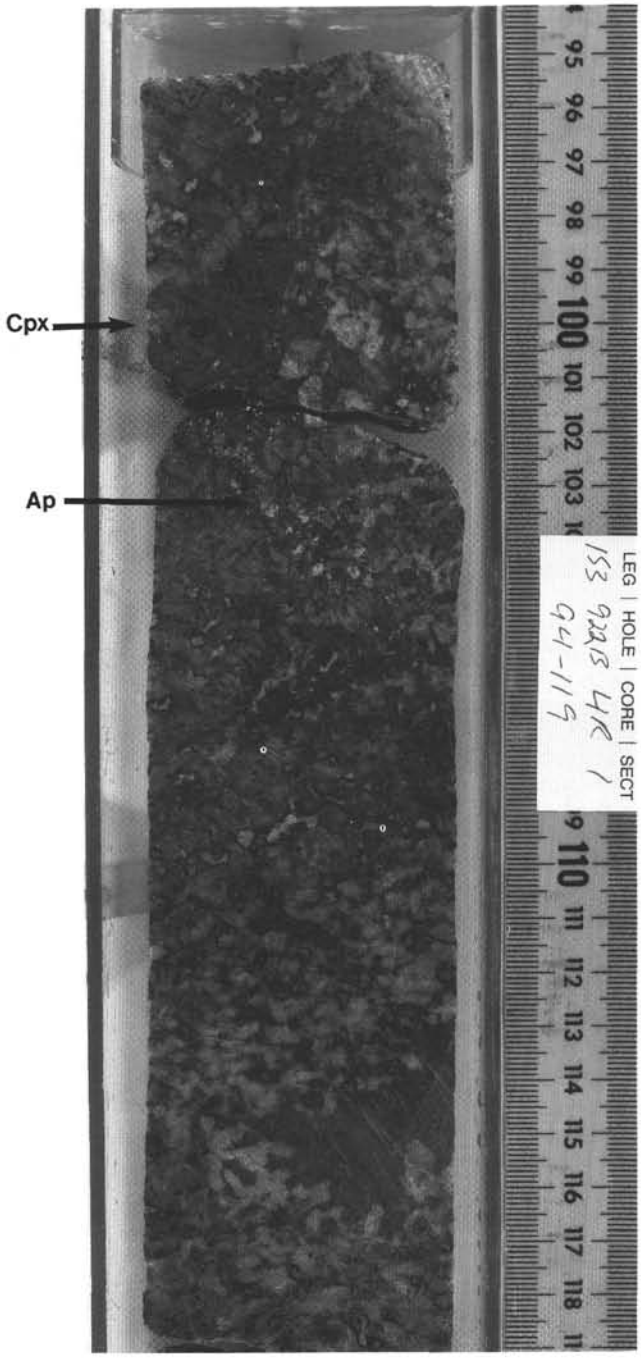

Figure 3. Olivine metagabbro with pegmatitic clinopyroxene (Cpx) and locally abundant apatite grains (Ap). The sample is cut by abundant narrow actinolite veinlets approximately 1 mm in width. (Sample 153-922B-4R-1, Pieces 8A and 8B, 94–119 cm).

saic texture. Plagioclase-rich zones are interlayered with anastomosing bands of hornblende and fine-grained oxide minerals and stringers, which are locally overprinted by fine-grained green amphibole. The hornblende-rich bands enclose porphyroclasts of olivine, aggregates of neoblastic fine-grained olivine, rounded to tapering porphyroclasts of clinopyroxene, and highly strained plagioclase grains. Retrograde alteration in these zones is commonly slight to moderate, with limited overprinting of actinolite-tremolite, talc, and minor chlorite. Local mylonitic intervals, which exhibit 80%–100% replacement, are typically related to densely veined and oxide-rich intervals with high-temperature alteration assemblages generally overprinted by lower temperature secondary phases of talc, actinolite, and minor chlorite.

Away from the shear zones, static metamorphism of the gabbroic rocks is heterogeneous and variable, both on a centimeter and several meter scale, reflecting variation in fracturing intensity and attendant hydration. Alteration intensities and occurrences of alteration minerals downhole and between holes is broadly similar; a consistent variation with depth is absent. Alteration intensities vary from slight to pervasive, and the highest intensities are associated with cataclastically deformed zones and intrusion of felsic veins. Interaction with the hydrothermal fluids resulted in static metamorphism under amphibolite to zeolite facies metamorphic conditions (Table 1). In general, background alteration is governed by replacement of olivine, followed by clinopyroxene and orthopyroxene, and disequilibrium textures are common. The earliest alteration phases typically occur along grain boundaries and fine veinlets and generally consist of fine-grained brown to pale-green amphibole.

Alteration of olivine is highly variable, and involves complex and heterogeneous coronitic replacement. Although alteration is locally pervasive, many samples contain up to 90% relict olivine. Initial stages of olivine alteration involve the formation of a microvein network containing fine-grained magnetite. With progressive alteration, talc and iron oxide minerals line the microfractures and develop discontinuous rims around grain boundaries. In more highly altered grains, irregular to concentric zonation replacement of olivine by secondary phases includes variable amounts of talc, magnetite as very fine grains and as "feathery" to dendritic intergrowths, mixed-layer chlorite smectite, Ca-Al amphibole, and cummingtonite. Locally, carbonate minerals occur as fine grains within the coronas and discontinuously rim corona margins. Where olivine is completely replaced, the talc and magnetite assemblage is generally absent and alteration is dominated either by intergrown chlorite and tremolite that form distinctive amoeboid-shaped felted patches, or by pods of smectite, pyrite, and chlorite. Where olivine grains are in contact with plagioclase, highly zoned, riming bands of pale-green chlorite with anomalous blue to olive-green birefringence are common. Olivine grains are commonly cut by arrays of vapor-rich fluid inclusions.

Clinopyroxene grains exhibit variable degrees of alteration; the most intensely altered grains typically occur in micropegmatitic patches and adjacent to felsic veins. Magnesiohornblende as fine-grained inclusions in clinopyroxene is common. With increasing alteration, fibrous rims of actinolitic hornblende and associated fine-grained oxide minerals form. The secondary amphibole is the most common hydrothermal mineral in the gabbroic rocks, replacing olivine, clinopyroxene, and plagioclase. Felted actinolitic mats and intergrown chlorite, with coronitic rims of chlorite after clinopyroxene, are most common in alteration halos associated with veins. In localized patches, as well as in micropegmatitic zones and in the cores of trondhjemitic to dioritic veins, hydrothermal clinopyroxene forms as turbid to clear irregular patches on primary clinopyroxene and as monomineralic grains. The pyroxene is distinguished petrographically from strictly magmatic pyroxenes by its pale-green color, an absence of exsolution lamellae, and ubiquitous primary fluid inclusions. The fluid inclusion-rich clinopyroxenes are similar to those in gabbroic rocks recovered from the other areas of MARK (Kelley and Delaney, 1987; Gillis et al., 1993; Kelley et al., 1993), from Hole 735B on the Southwest Indian Ridge (Stakes, 1991; Stakes et al., 1991; Kelley et al., 1993), and Hess Deep (Gillis, 1996).

Orthopyroxene alteration intensity is highly variable, ranging from moderate to pervasive, and finer grains are generally more pervasively altered. Cummingtonite and fine-grained oxide minerals typically fill microfractures cutting orthopyroxene grains, form narrow rims around the grains, and occur as isolated fibrous patches within the grains.

Alteration of plagioclase ranges from <10% to 100% and predominantly involves the formation of secondary plagioclase, with lesser

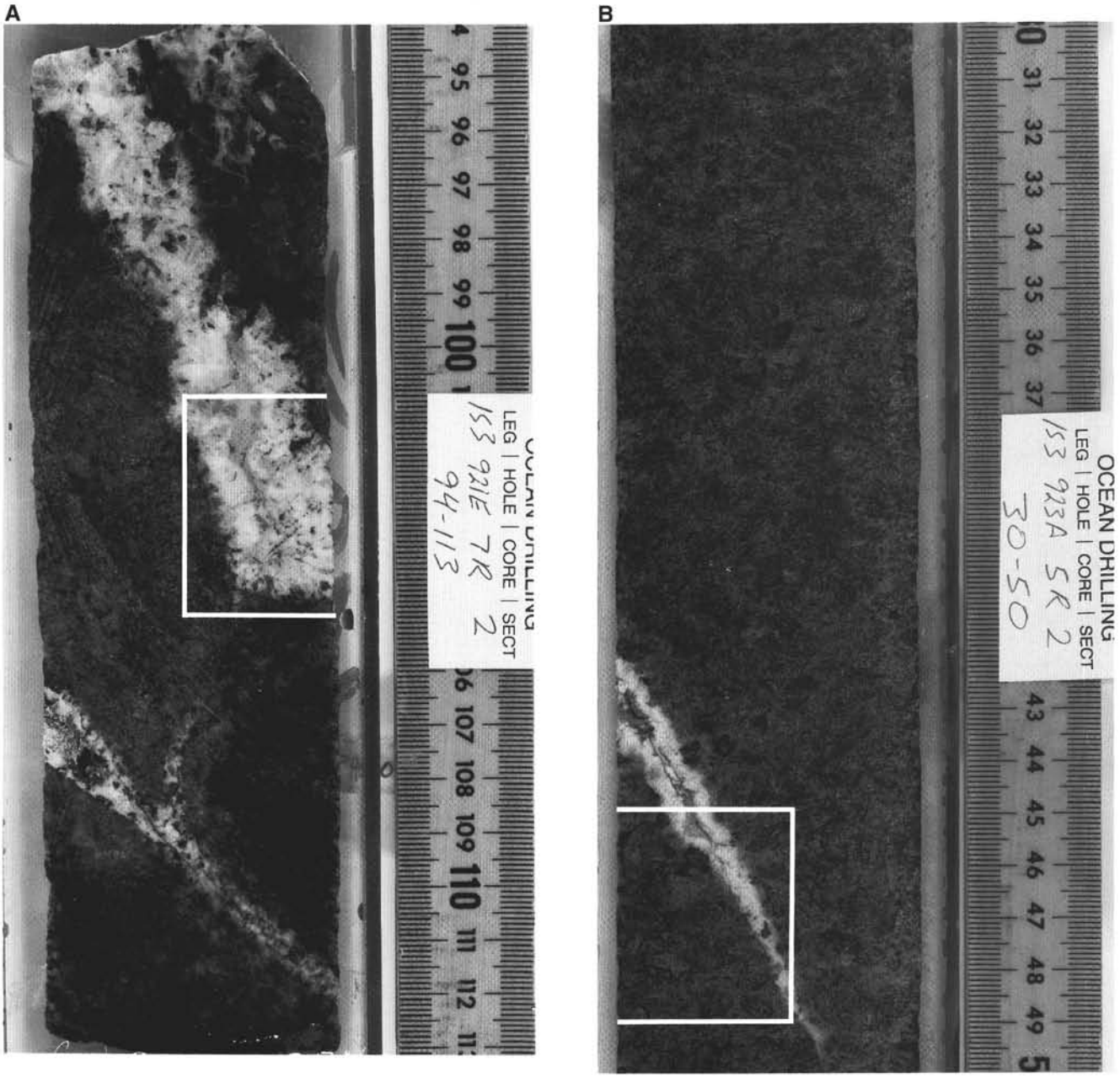

Figure 4. **A.** Complex olivine gabbro and oxide gabbro cut by a trondhjemitic vein composed of highly altered plagioclase, quartz, and amphibole, with minor hydrothermal clinopyroxene. The narrow vein at the top of the piece contains altered plagioclase and bladed to prismatic, euhedral, brown amphibole, and elongated crystals of amphibole. Moderately well developed alteration halos form rims that are 5–10 mm wide and are composed of variable amounts of actinolite, chlorite, and secondary plagioclase with minor epidote. Note the narrow felsic veinlet that connects the two larger veins (Sample 153-921E-7R-2, Piece 4, 94–113 cm). **B.** Slightly altered gabbro that is cut by a composite vein with an amphibole- and clinopyroxene-rich core and plagioclase + quartz rim (Sample 153-923A-5R-2, Piece 1, 30–50 cm). Outlined area on sections denotes where sample was taken for fluid inclusion analyses.

amounts of actinolite, chlorite, epidote, prehnite, zeolite, and clay minerals. Alteration is most intense adjacent to crosscutting veins and vein networks, within cataclastic deformation zones, and in felsic veins and associated alteration halos in the bounding host rock. Locally, in extensively altered patches the plagioclase is turbid and dusty in appearance owing to replacement by secondary plagioclase, clay, and zeolite minerals. In these zones, the secondary plagioclase is characterized by the presence of abundant anhedral to euhedral, liquid-dominated fluid inclusions. Fine-grained, fibrous sprays of actinolite intergrown with chlorite commonly rim grain boundaries and fill microfractures that crosscut the plagioclase grains. In the micropegmatitic zones and in felsic veins and associated alteration halos, epidote as well as prehnite are locally abundant.

The most abundant type of veins in the plutonic rocks from Sites 921 to 923 comprise an irregular microscopic network of actinolitic veins, which rim grain boundaries and overprint high-temperature deformation fabrics (see Dilek, Kempton, et al., this volume). This fracture system most likely facilitated fluid flow into the gabbroic sequence, resulting in the background alteration. Macroscopic veins are most commonly composed of actinolite and chlorite, with rare, later veins filled by variable amounts of chlorite, smectite, prehnite, epidote, and actinolite. Alteration in intensely deformed zones associat-

Table 1. Metamorphic summary, Sites 921–923.

Lithology	Mineralogy		Fluids
	Primary	Secondary	
Gabbro	Olivine	Heterogeneous coronitic replacement, tremolite-actinolite, talc, chlorite-smectite, magnetite, carbonate, pyrite	CO_2-CH_4-H_2O
	Clinopyroxene	Secondary clinopyroxene, brown amphibole, actinolite, chlorite, magnetite	H_2O-NaCl
	Orthopyroxene	Cummingtonite, talc, chlorite, smectite, magnetite	
	Plagioclase	Secondary plagioclase, actinolite, chlorite, epidote, prehnite, clay	H_2O-NaCl, CH_4-$H_2O \pm H_2$
	Apatite		CO_2, CO_2-CH_4(?)-H_2O, CO_2-$H_2O \pm$ brine, H_2O-NaCl
	Titanomagnetite	Ilmenite, titanite, carbonate	
	Quartz		H_2O-NaCl, H_2O-NaCl-brine
	Vein types		
Magmatic:	Plagioclase, quartz, amphibole, hydrothermal clinopyroxene		
Hydrothermal:	Actinolite, chlorite, prehnite, epidote, clay, smectite		
Alteration intensity:	<5%–100% altered		
Metamorphic facies:	Granulite to zeolite		

ed with cataclastic deformation and in net-veined zones is commonly pervasive. Static alteration of the late-stage trondhjemitic to dioritic veins that cut the core is generally moderate to pervasive (Fig. 4). The felsic veins are typically zoned and are characterized by clinopyroxene and amphibole-rich cores, and plagioclase and quartz-rich margins. They commonly contain accessory phases of apatite, zircon, and iron oxide minerals (Fig. 3). The veins are submillimeter to several centimeter in scale, exhibit sharp to diffuse contacts, and moderately to well-developed alteration halos (Fig. 4). Primary minerals within the veins and in the bounding wall rock are highly to pervasively replaced by variable amounts of actinolite, chlorite, talc, hydrothermal clinopyroxene, secondary plagioclase, prehnite, and epidote. Brown hornblende is common along the vein margins where it rims clinopyroxene and olivine in the host rock. Plagioclase adjacent to the margins is turbid in appearance due both to abundant fine-grained inclusions of clay? and liquid-dominated fluid inclusions. Oxide minerals are replaced by titanite and are locally enclosed in fibrous intergrowths of actinolite and chlorite.

FLUID INCLUSIONS

Methods

Microthermometric analyses of fluid inclusions were conducted on a Fluid Inc. adapted U.S. Geological Survey gas-flow heating and freezing stage according to the procedures outlined by Roedder (1984). Replicate homogenization and freezing measurements were carried out on individual inclusions to obtain corresponding homogenization temperatures and fluid salinities. Homogenization and dissolution temperatures were measured during progressive heating of the sample to avoid decrepitation and potential alteration of phase change temperatures because of stretching and leaking. To obtain a representative sampling of inclusion populations, each reported analysis of homogenization temperature and corresponding inclusion composition represents measurements of a subpopulation of four to five individual inclusions along an array of inclusions, or of a cluster of primary inclusions. Except for inclusions trapped under immiscible conditions, inclusions along individual microfractures or primary clusters homogenized within 5°–10°C of adjacent inclusions. The fluid inclusion stage was calibrated by presetting the instrument to yield temperatures of phase transitions of synthetic fluid inclusions at −56.6°C, 0.0°C, and +374°C. All analyses were reproducible to within 0.1°C. Unsaturated and saturated salinities were obtained using the equations of Zhang and Frantz (1987) and are reported in terms of NaCl equivalent. Fluid compositions of the CH_4-H_2O-bearing inclusions, using clathrate melting and homogenization temperatures, were obtained using the data of Zhang and Frantz (1992). Melting temperatures of CH_4 clathrates were obtained by temperature cycling close to the final clathrate melting temperature (Seitz and Pasteris, 1990). The volatile components of fluid inclusions were confirmed by micro-Raman analyses conducted at the Carnegie Geophysical Laboratory, Washington, D.C., using a Dilor® XY conofocal micro-Raman system equipped with an EG & G® Model 1433-C cryogenic CCD detector. Gases were identified by their Raman bands: e.g., CH_4 ($\upsilon_1 \sim 2917\ cm^{-1}$), CO_2 ($2\upsilon_2 \sim 1388\ cm^{-1}$), and H_2 ($Q_1 \sim 4155\ cm^{-1}$) (Schrotter and Klockner, 1979; Herzberg, 1951). Abbreviations for inclusion homogenization behavior are as follows: (Th L + V [L]) indicates the temperature of homogenization for liquid [L] + vapor [V] inclusions that homogenize to the liquid phase (i.e., by disappearance of the vapor bubble); (Th L + V [V]) indicates the apparent temperature of homogenization for liquid + vapor inclusions that homogenize by expansion of the vapor bubble; (Tm < Th L + V [L]) indicates the temperature of homogenization for halite-bearing inclusions in which halite dissolution occurs before vapor bubble disappearance and that the inclusions homogenize into the liquid phase; and (Tm > Th L + V [L]) indicates the temperature of homogenization for halite-bearing inclusions in which halite dissolution occurs subsequent to vapor bubble disappearance.

FLUID INCLUSION TYPES AND RESULTS

Fluid inclusion types were described and classified petrographically at room temperature previous to microthermometric analyses. Fluid inclusions in the plutonic rocks from Sites 921 to 923 are common in gabbroic matrix minerals as secondary inclusions along healed microfractures. They occur less commonly as primary inclusions trapped during the growth of magmatic and alteration mineral phases. The inclusions are most abundant in apatite and quartz within micropegmatitic pods, in oxide gabbros, and in late-stage felsic veins. Primary inclusions in apatite occur as tubular, euhedral inclusions oriented parallel to crystal faces; however, in some apatite and quartz grains inclusions are so abundant that it is impossible to unambiguously determine their origin (Tables 1, 2). Secondary fluid inclusions along healed microfractures are especially common in plagioclase and quartz, although they also occur in apatite, epidote, and amphibole. Based on petrographic analyses at room temperature, the inclusions were classified into four main types; results of microthermometric analyses of these inclusions and their host rock types and host minerals are presented in Table 2.

Type 1. Liquid-Dominated Inclusions

Gabbroic- and vein-hosted, liquid-dominated to vapor-rich fluid inclusions are pervasive in plagioclase and quartz, and less common in apatite, epidote, and amphibole (Fig 5A; Table 2). Only plagio-

Table 2. Analyses of fluid inclusions, Holes 921-924.

Sample	Depth (mbsf)	Rock type	Mineral host	Or	Th (°C)	Avg	s.d.	Ph	Tm (°C)	Avg	s.d.	NaCl wt%	Avg	s.d.	Comments
921E-7R-2 (Piece 4, 101–105 cm)	61.82	Trondhjemitic vein in gabbro	Quartz	P/S	316–335 (6)	325	7.4	L	+311 to +327	319	5.9	39–40	39.7	0.5	H_2O + NaCl
			Quartz	P/S	270–319 (20)	290	15.2	H	+295 to +348	321	13.4	38–42	49.8	1.1	H_2O + NaCl
			Quartz	P/S	277–400 (48)	310	26.8	L	–0.8 to –6.6	2.7	1.2	1.3–10.0	4.4	1.8	H_2O + NaCl
921E-8R-1 (Piece 13A, 109–113 cm)	70.09	Trondhjemitic vein in gabbro	Quartz	S	264–304 (37)	286	11.4	L	–0.8 to –5.2	3.0	0.8	1.3–8.1	4.8	1.2	H_2O + NaCl
		Gabbroic host	Plagioclase	S	273–314 (26)	303	9.5	L	+0.2 to +2.6	1.5	0.7				H_2O + CH_4(?)
922A-3R-1 (Piece 3B, 36–40 cm)	13.86	Deformed oxide gabbro	Apatite	P*	22*(18)			V	–56.6	–56.6					CO_2
923A-5R-2 (Piece 1, 45–49 cm)	24.36	Trondhjemitic vein in olivine	Quartz	S	335–429 (14)	386	30.4	L	+325 to +360	343.6	14.1	40–44	41.8	1.3	H_2O + NaCl
		Gabbronorite	Quartz	S	331–350 (2)	340.5	13.4	H	+342 to +355	348.9	0.8	42–43	42.3	0.8	H_2O + NaCl
			Quartz	P/S	290–342 (26)	320	13.2	L	–4.3 to –17	8.2	3.6	6.8–20.2	11.6	3.8	H_2O + NaCl
			Plagioclase	S	297–320 (3)	310	11.7	L	+1.0 to –1.2	1.1	0.1				CH_4 + H_2O
923A-7R-2 (Piece 3, 41–45 cm)	28.69	Olivine gabbro	Apatite	P/S	172–314 (30)	271	38	L	–2.4 to –10.5	6.4	2.0	3.9–14.5	9.6	2.6	H_2O + NaCl)
			Apatite	P/S	356–375 (3)	367	10	L	+4.0 to +6.6	5.7	1.5				CO_2 ± CH_4(?) + H_2O
			Apatite	P/S	301–378 (7)	362	28	V	+5.6 to +8.2	6.7	1.0				CO_2 ± CH_4(?) + H_2O
			Plagioclase	S	293–341 (22)	324	18	L	–1.4 to –4.7	2.1	1.0	2.3–7.4	3.5	1.6	H_2O + NaCl
923A-10R-1 (Piece 5A, 72–74 cm)	37.22	Trondhjemitic vein in olivine gabbro	Quartz	P/S	219–245 (13)	242	17.7	H	+318 to +495	377.8	47	40–59	45	5.3	H_2O + NaCl
			Quartz	S	287–318 (20)	308	10.1	L	–1.7 to –12.6	5.8	2.3	2.8–16.5	8.3	3.0	H_2O + NaCl
			Quartz	S	397–408 (4)	402	6.4	V	–0.8 to –1.0	0.9	0.1	1.3–1.6	1.5	0.2	H_2O + NaCl
923A-12R-1 (Piece 5B, 110–115 cm)		Olivine gabbro	Plagioclase	S†	349–365 (25)	356	4.8	L	+9.4 to +10.7	10.1	0.4				CH_4 + H_2O

Notes: Or = inclusion origin; P = primary; S = secondary; Th (°C) minimum–maximum temperature = homogenization temperature range, ( ) = number of inclusions measured; Avg = average; s.d. = standard deviation; Ph = phase to which inclusions homogenize; L = liquid; V = vapor; c = critical behavior; Tm (°C) = melting temperature range of ice, solid, or clathrate; NaCl wt% = NaCl wt% equivalent. * = inclusions freeze at –90°C to –100°C. † = solid melting event at –180°C, corresponding to melting of methane.

clase-, apatite-, and quartz-hosted inclusions were measured in this study. In plagioclase and apatite, these low-temperature inclusions commonly exhibit negative to irregular crystal habits and form anastomosing arrays along healed microfractures. In quartz, some inclusions are clearly secondary, however, more commonly the inclusions are so abundant that it is impossible to unambiguously determine a primary or secondary origin. In highly altered zones, which typically occur adjacent to late-stage magmatic veins and within the veins, concentrated zones of irregularly shaped inclusions that are believed to be primary in origin occur in turbid patches of secondary plagioclase. Liquid-dominated inclusions in plagioclase homogenize to the liquid phase (Th L + V [L]) at temperatures of 293°–341°C and contain equivalent salinities of 2.3–7.4 wt% NaCl (Tables 1, 2; Figs. 6–9). Apatite-hosted inclusions homogenize to the liquid phase at temperatures of 172°–314°C and contain equivalent fluid salinities of 2.4–10.5 wt% NaCl (Table 2; Figs. 6–9). Liquid-dominated to vapor-rich fluid inclusions in quartz homogenize to the liquid phase at temperatures of 264°–400°C and contain equivalent fluid salinities of 1.3–20.2 wt% NaCl.

Type 2. Vapor-Dominated Inclusions

Vapor-dominated inclusions are common in apatite, olivine, and hydrothermal clinopyroxene, and less common in quartz (Fig. 5B; Tables 1, 2). In apatite and clinopyroxene, these inclusions are clearly primary and secondary in origin. In quartz, however, it is commonly difficult to determine their origin because of the extreme abundance of inclusions in these grains. Apatite-hosted inclusions were analyzed in this study, as were rare, quartz-hosted inclusions. Apatite-hosted, vapor-dominated inclusions occur as two types. The first type are primary inclusions that are commonly completely vapor-filled at room temperature and that typically remain so on cooling; rare inclusions homogenize on warming to the vapor phase at temperatures of +22°C. The inclusions exhibit first solid melting temperatures at –56.6°C (Table 2) and exhibit a freezing event at temperatures of –90° to –100°C. The phase transitions indicate that the fluids are dominated by CO_2. The second type of vapor-dominated inclusions are both primary and secondary in origin. They homogenize to the vapor phase (Th L + V [V]) at temperatures of 301°–378°C and exhibit clathrate melting temperatures of +5.6° to +8.2°C (Table 2). Some inclusions, however, that are petrographically similar homogenize to the liquid phase at temperatures of 356°–375°C and exhibit clathrate melting temperatures of +4.0° to +6.6°C. Similar inclusions are observed in gabbroic rocks from both the MARK area and from Hole 735B, where micro-Raman analyses indicate that these inclusions are CO_2-H_2O-dominated (Kelley et al., 1993; Kelley, 1996). The behavior of inclusions from Sites 921 to 923 is consistent with fluids that are dominantly CO_2-H_2O; however, they may also contain small concentrations of volatile species such as CH_4 as well. Strong fluorescence during preliminary micro-Raman analyses of these inclusions precluded determining the volatile species.

Rare vapor-dominated inclusions in quartz (Sample 153-923A-10R-1, Piece 5A, 72–78 cm) homogenize to the vapor phase at temperatures of 397°–408°C, and contain fluids with 1.3–1.6 wt% NaCl equivalent salinities (Tables 1, 2; Figs. 6–9). These inclusions do not show evidence of clathrate formation on warming, indicating that they are most likely dominated by low-salinity aqueous fluids.

Type 3. Daughter-Mineral-Bearing Inclusions

Halite-bearing inclusions are rare in gabbroic rocks from Sites 921 to 923, but they are common in trondhjemitic to dioritic veins that cut the gabbros (Figs. 4, 5C; Table 2). In the gabbroic rocks, halite-bearing inclusions occur in matrix apatite and, more rarely, in quartz in localized shear zones. Halite-bearing inclusions are most abundant in quartz grains within the felsic veins, where they occur as secondary inclusions; however, in many grains, inclusions are so abundant that an unequivocal origin of the inclusions cannot be de-

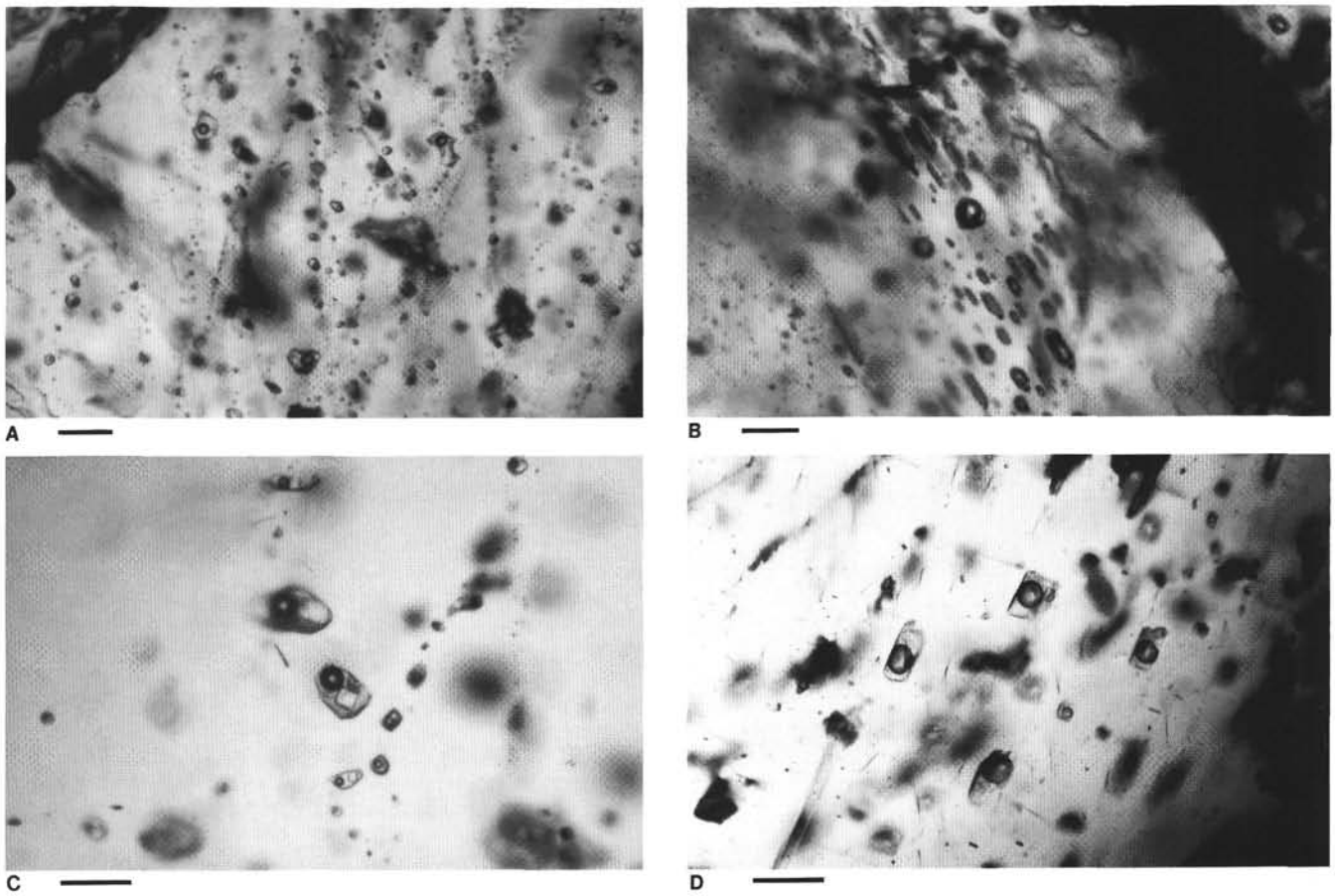

Figure 5. Photomicrographs of fluid inclusion types 1 and 3. **A.** Type 1, quartz-hosted, liquid-dominated inclusions along healed microfractures. **B.** Type 2, vapor-dominated, CO_2-rich fluid inclusions in apatite. **C.** Type 3, halite-bearing fluid inclusion in quartz. The brine-rich inclusions contain a moderate-sized vapor bubble rimmed by a high-salinity liquid and a halite daughter mineral. **D.** Type 4, CH_4-H_2O-bearing, vapor-rich fluid inclusion in plagioclase. Scale bar in all photos is equal to 15 μm.

termined. Halite daughter minerals that contain an opaque cubic daughter mineral, tentatively identified as pyrite, are rare. The liquid-dominated to vapor-rich brine inclusions exhibit three types of homogenization behavior on heating. Inclusions that homogenize by vapor bubble disappearance at temperatures of 316°–429°C and exhibit halite dissolution temperatures of 311°–360°C contain fluid salinities of 39–44 wt% NaCl equivalent. Fluids in these inclusions lie in the field just to the right of the liquid + vapor + halite curve (L + V + H) shown in Figure 6 and to the right of the dashed line in Figure 10. Halite-bearing inclusions that have entrapped fluids that plot on the gently sloped curve shown in Figures 6 and 7, and that fall in the field to the left of the dashed line in Figure 10, homogenize by halite dissolution (Tm > Th L + V [L]) at temperatures of 295°–495°C and disappearance of the vapor bubble occurs at 219°–350°C. These inclusions contain equivalent fluid salinities of 38–59 wt% NaCl. Inclusions that contain fluids that exhibit simultaneous halite dissolution and vapor bubble disappearance lie on the 1:1 dashed line shown in Figure 10.

Type 4. CH_4-H_2O ± H_2–Bearing Inclusions

Vapor-rich and complex daughter-mineral-bearing inclusions in plagioclase are common throughout the gabbroic sequence (Fig. 5D). The vapor-rich inclusions exhibit first solid melting temperatures at −180°C, clathrate melting temperatures of +9.4° − +10.7°C, and homogenize by vapor bubble disappearance at temperatures of 349°–365°C (Fig. 11; Tables 1, 2). Rare inclusions exhibit critical behavior on warming. Phase relationships of these inclusions indicate that they are dominated by CH_4-H_2O and that they contain up to about 11 mol% CH_4. Petrographically similar inclusions in Samples 153-921E-8R-1 (Piece 13A, 109–113 cm), and 153-922A-7R-2 (Piece 3, 41–45 cm), exhibit clathrate melting temperatures of +0.2° to +2.6°C, but these inclusions do not exhibit a solid melting event at −180°C. Homogenization temperatures of inclusions in these two samples range from 273°–320°C. The inclusions most likely also contain CH_4-H_2O. Preliminary micro-Raman spectroscopic analyses of the plagioclase-hosted inclusions confirm that CH_4 is the dominant volatile species in some of the vapor-rich inclusions and that they contain molecular H_2 as well. The CH_4-H_2O ± H_2 inclusions are similar to inclusions in gabbroic rocks recovered from the Southwest Indian Ridge at Hole 735B (Vanko and Stakes, 1991; Kelley et al., 1994; Kelley, 1996) and in samples recovered by *Alvin* near Sites 921–924 (Kelley et al., 1993; Kelley, 1996). In submarine systems, H_2 has only previously been recorded in plutonic-hosted inclusions from Hole 735B (Kelley, 1996; Kelley and Früh-Green, 1995).

DISCUSSION

In the gabbroic rocks recovered from MARK, penetrative magmatic fabrics and complex mineral chemistry, along with overprinting secondary mineral phases, compositionally and thermally distinct populations of fluid inclusions, and crosscutting vein networks, indicate that the plutonic sequence underwent multiple magma-hydro-

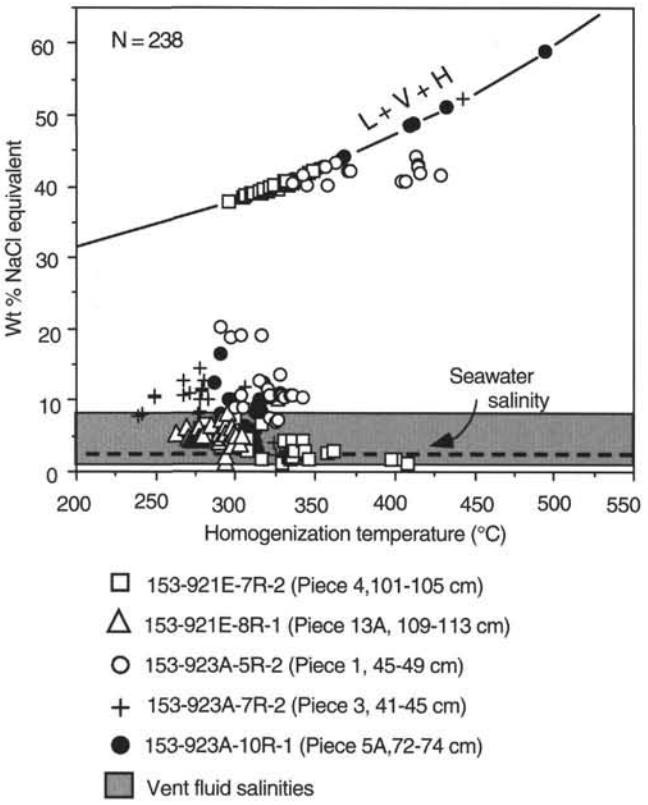

Figure 6. Uncorrected homogenization temperatures and corresponding equivalent fluid salinities for plutonic-hosted inclusions from Sites 921 to 923. N corresponds to the number of inclusions measured.

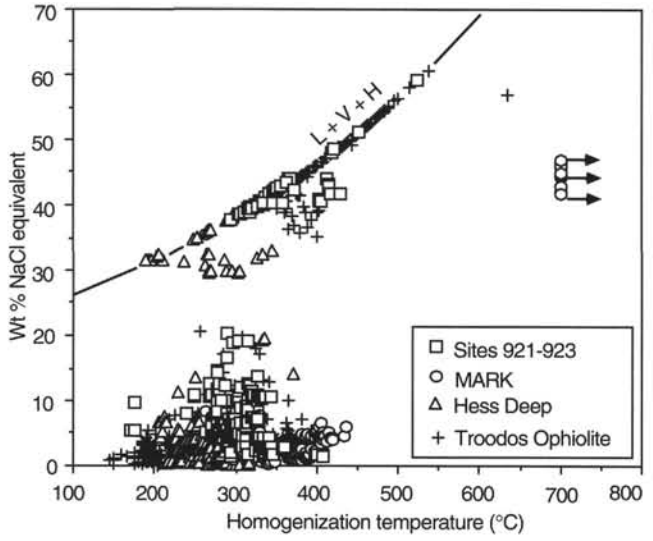

Figure 7. Corresponding homogenization temperatures and equivalent fluid salinities of plutonic-hosted fluid inclusions in submarine environments. The primary(?) and secondary inclusions in the plutonic rocks from Sites 921 to 923 exhibit a compositional evolution that is similar to that observed in gabbros and trondhjemitic rocks previously recovered from the MARK area, to gabbroic rocks recovered from Hess Deep at ODP Site 894, and to upper level gabbroic and plagiogranitic rocks from the Troodos ophiolite. Arrows indicate that high-salinity apatite-hosted inclusions remain unhomogenized at temperatures of 700°C.

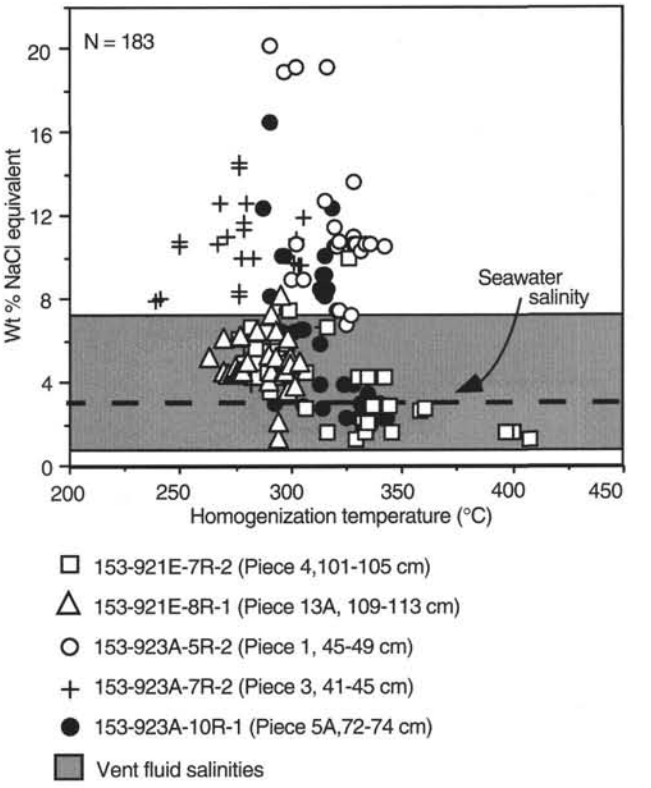

Figure 8. Uncorrected homogenization temperatures and corresponding fluid salinities for low-salinity, gabbro- and vein-hosted inclusions from Sites 921 to 923. Fluid inclusions in trondhjemitic to dioritic veins that cut the gabbroic rocks record some of the highest salinity fluids reported for deep-seated submarine hydrothermal systems.

thermal pulses as the rocks cooled and were transported away from the zone of crustal accretion. The distribution and spatial evolution of fluids associated with these high-temperature plutonic environments is poorly known; however, as more of these systems are explored some general mineralogical-compositional relationships are emerging that provide a working model with which to examine magmatic and hydrothermal fluid evolution through the subsolidus regime to hydrothermal seawater-dominated conditions. In the following discussion, an overview of this model that is based on integrated experimental, theoretical, and fluid inclusion analyses is presented. Fluid inclusion data from Sites 921 to 923 are evaluated below in the context of this model.

Evolution of Magmatic Volatiles

Analyses of occluded gases in basaltic glasses coupled with solubility data indicate that, because of the low solubility of CO_2 in basaltic melts, mid-ocean ridge basalts (MORBs) are saturated or oversaturated with respect to CO_2, with typical concentrations of <400 ppm (Delaney et al., 1978; Fine and Stolper, 1986; Dixon et al., 1988; Stolper and Holloway, 1988; Pawley et al., 1992). In contrast, the incompatible nature of H_2O, coupled with its low concentration, means that melts are generally undersaturated with respect to H_2O, with concentrations typically < 5000 ppm (Moore, 1977; Delaney et al., 1978; Dixon et al., 1988). Under shallow crustal conditions, compositionally evolved interstitial melts may become saturated with respect to water: however, for a mid-ocean ridge basaltic melt emplaced 2–3 km beneath a ridge axis, this does not occur until approximately >95% crystallization (Burnham, 1979). Such conditions are probably not achieved until temperatures of ~700°–800°C (Wyllie, 1977; Burnham, 1979). The salinity of the exsolved aqueous phase is controlled

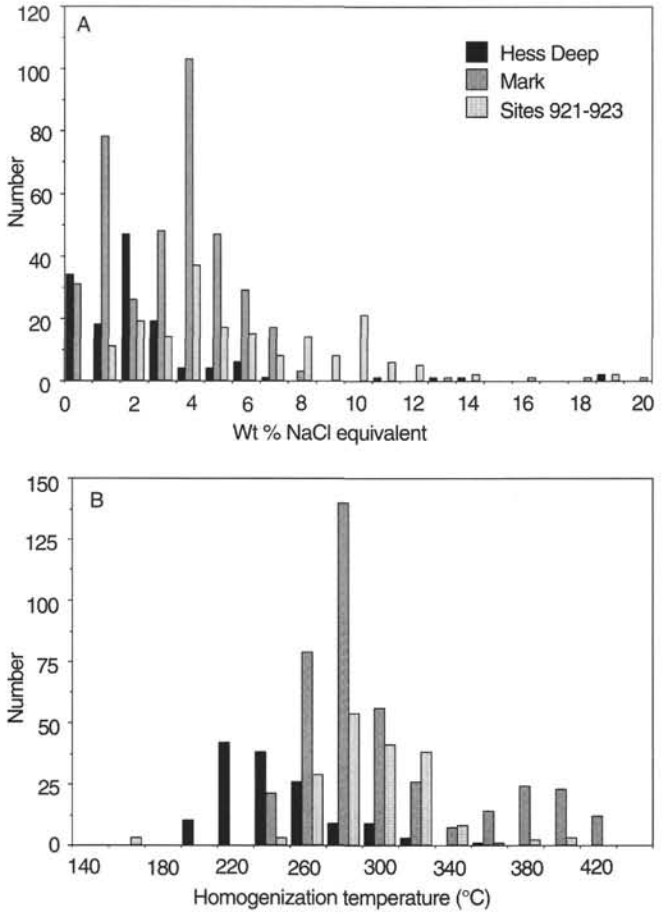

Figure 9. Histograms of fluid inclusion salinities **(A)** and uncorrected homogenization temperatures **(B)** for plutonic samples from Sites 921 to 923, those previously collected from MARK, and from Site 894 at Hess Deep.

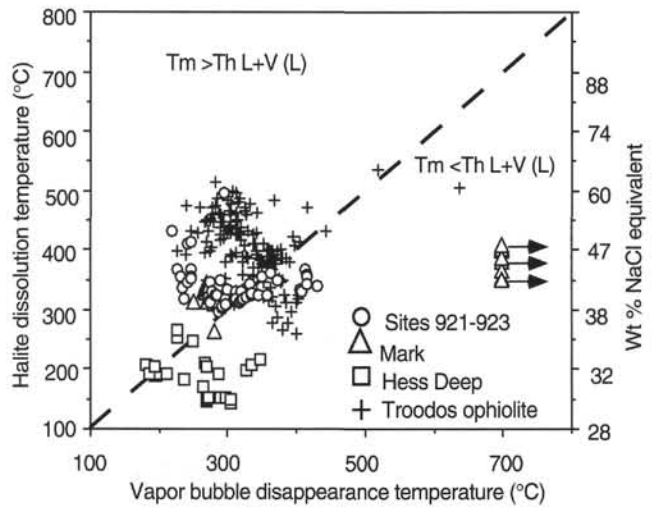

Figure 10. Corresponding vapor bubble disappearance temperatures and halite dissolution temperatures for halite-bearing inclusions in gabbroic rocks from Sites 921 to 923, in gabbroic and rare trondhjemitic rocks previously collected from MARK near Sites 921–924, in gabbroic rocks from Hess Deep at Site 894, and from upper level gabbroic and plagiogranitic rocks from the Troodos ophiolite, Cyprus.

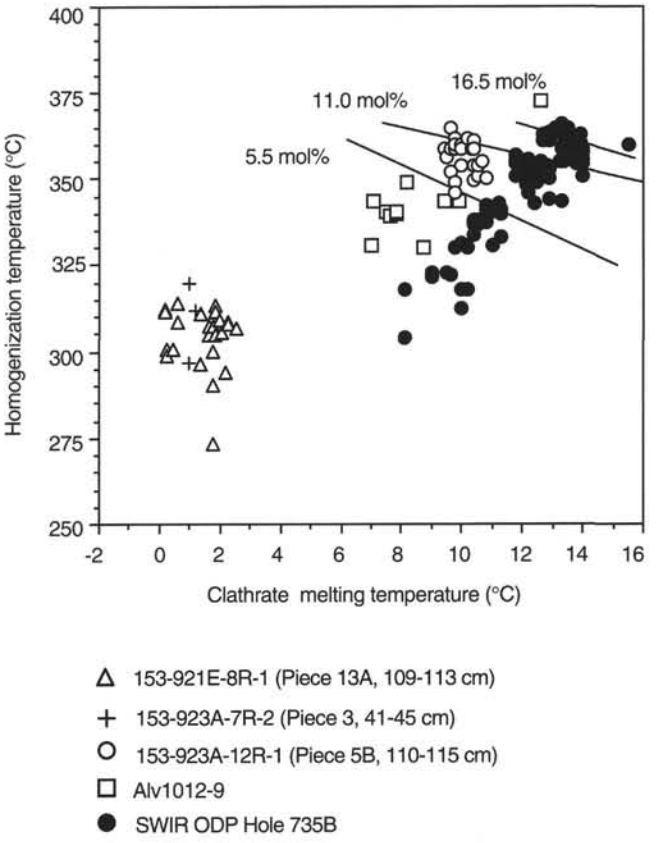

Figure 11. Corresponding clathrate melting and homogenization temperatures for CH_4-bearing inclusions. Melting and homogenization temperatures of the secondary inclusions from Sites 921 to 923 indicate that the inclusions contain up to ~11 mol% CH_4. These inclusions are similar to those in gabbroic rocks from the Southwest Indian Ridge recovered from Hole 735B, and to those in gabbroic rocks previously collected from MARK (i.e., *Alvin* sample ALV1012-9). Experimentally derived isopleths are after Zhang and Frantz (1992).

by the chlorine content of the melt and the partition coefficient between the melt and the volatile phase. Depending on the initial bulk composition of these evolved fluids, and the temperature and pressure under which volatile exsolution occurs, fluids may be exsolved from the melt as either immiscible (i.e., vapors and brines) or homogeneous phases. Experimental work by Frantz et al. (1992), that examines the compositional limits of immiscibility in the CO_2-H_2O-NaCl system from 500°–700°C and at pressures of 1–3 kbar shows that exsolution of late-stage volatiles is most likely to occur under immiscible conditions in submarine magma chambers in shallow crustal environments. Compositions of the vapors and brines formed during supercritical phase separation (condensation) are dependent only on the temperature and pressure at which immiscibility occurs and are independent of the parental fluid salinity (see Fournier, 1987, for a more detailed discussion).

In highly evolved and H_2O-rich systems such as those in backarc spreading environments, the latest fluids may involve direct exsolution of brines formed in the absence of a vapor phase. Theoretical modeling of fluid evolution in silicate melts indicates that highly saline fluids may be exsolved from late-stage melts in shallow crustal environments (Cline and Bodnar, 1991). At pressures of 0.5–1.0 kbar, exsolving fluids are incapable of removing substantial amounts of chlorine from the melt, and thus, chlorine concentrations in the melt increase as crystallization proceeds. Assuming isothermal crystallization of silicic melts at 700°C and an initial Cl/H_2O ratio of 0.1, fluid salinities evolve from 1–7 wt% NaCl, as the first fluids exsolve,

to 80–90 wt% NaCl, at high degrees of crystallization (Cline and Bodnar, 1991). As a result of the partitioning of H_2O and chlorine in the melt, at pressures of 2 kbar or greater, this evolution is reversed and fluids evolve from highly saline brine to low-salinity fluids. The exact compositions of these fluids will depend on the initial volatile and chlorine contents of the melts, as well as on the T-fO_2 path, but the general trend in fluid composition should hold true for late-stage magmatic fluids in submarine settings as well. It should be noted that, for most mid-ocean ridge systems, it is unlikely that brines generated either by supercritical phase separation of magmatic fluids or by direct exsolution are volumetrically significant because of the incompatible nature and low concentrations of H_2O in basaltic melts. From these data it may be predicted that the progressive degassing of fluids in shallow submarine crustal environments will result in the following general compositional evolution:

decreasing temperature →

$$CO_2 \rightarrow CO_2 + H_2O[V] + H_2O \pm CO_2 + \text{Brine}[L] \rightarrow \text{Brine}.$$

Fluid Evolution in Plutonic Rocks from Sites 921 to 923

The mineralogy and textures of the gabbroic samples recovered from MARK indicate that the rocks crystallized predominantly from tholeiitic magma (see Casey, this volume). However, in isolated pockets and veins, represented by the pegmatitic gabbros, oxide gabbros, and trondhjemitic to dioritic veins, considerable chemical evolution/ modification occurred in the later stages of the crystallization history. In these rocks, the occurrence of accessory minerals such as apatite, zircon, oxide minerals, and amphiboles that are texturally primary in origin, are consistent with crystallization of these phases under relatively high fO_2 and from a hydrous magma (Pedersen and Malpas, 1984; Pedersen, 1986; Kelley and Malpas, 1996). Analyses of primary fluid inclusions in magmatic apatite in these evolved pods show that the earliest fluids to be exsolved from the melts are dominated by CO_2-rich vapor, which with progressive fractionation evolved to more H_2O-rich compositions. The CO_2- and CO_2-H_2O-rich fluids are not unique to mid-ocean ridge gabbros as they have been observed in gabbros previously collected from the MARK area near Sites 921–924 (Kelley and Delaney, 1987; Kelley et al., 1993), in gabbroic rocks from Hole 735B (Kelley, 1996), from gabbroic to trondhjemitic rocks at Site 894 at Hess Deep (Kelley and Malpas, 1996), and in a metagabbro sample from the Oceanographer Transform (Vanko et al., 1992). In the samples collected by *Alvin* from the MARK area and the Oceanographer Fracture Zone, the low-density CO_2-H_2O-rich vapors are associated with brines containing 40–50 wt% NaCl ± $CaCl_2$. The presence of coexisting vapors and brines in these samples provides unequivocal evidence that they were entrapped under immiscible conditions, which in the MARK gabbros reflect temperatures >700°C, and pressures of approximately 1.2 kbar. These fluids are most common in micropegmatitic to pegmatitic pods and likely represent percolation of volatile-rich fluids through the gabbroic sequences late in their magmatic histories (Kelley and Malpas, 1996). In gabbroic rocks from Sites 921 to 923, rare halite-bearing inclusions that are spatially associated with CO_2-H_2O vapors most likely indicate that these fluids were exsolved under immiscible conditions from late-stage melts as well. Microthermometric analyses of the brine inclusions are in progress. The presence of CO_2-H_2O vapor-rich inclusions that occur along healed microfractures within the same apatite grains that host primary inclusions that are similar in composition suggests that these fluids were derived from the residual melts both during mineral growth, as well as during later high-temperature fracturing events. As condensation generates a volumetrically small amount of brine and a correspondingly large vapor component, it is not surprising that halite-bearing inclusions that are clearly associated with vapor-rich inclusions are rare in these rocks. Although formation of brines by condensation is widely regarded as the dominant mechanism for generating the extreme salinity variations of some fluids observed in submarine plutonic rocks and in vent fluids (Delaney et al., 1987; Kelley and Delaney, 1987; Vanko, 1988; Bischoff and Rosenbauer, 1989; Von Damm, 1990; Von Damm et al., 1992), accumulating evidence suggests that the exsolution of brines directly from late-stage melts may also play a significant role in formation of plutonic-hosted fluids. The ubiquitous occurrence of halite-bearing inclusions that homogenize by halite dissolution to the compositionally most evolved plutonic rocks from Sites 921 to 923 is similar to trondhjemitic-hosted inclusions from the MARK area (Kelley et al., 1993), to inclusions that occur throughout the upper level plutonic sequence of the Troodos ophiolite, Cyprus (Kelley et al., 1992), and to inclusions in pegmatitic patches in gabbroic rocks from Hole 894G at Hess Deep (Kelley and Malpas, 1996). In these plutonic suites, the observation that brine-rich inclusions that homogenize predominantly by halite dissolution consistently occur only in the most compositionally evolved rocks, coupled with the virtual absence of vapor-dominated inclusions, is consistent with brine exsolution from late-stage melts in the absence of a vapor phase. In the plutonic rocks from Sites 921 to 923, secondary arrays of inclusions with salinities of 38–59 wt% NaCl equivalent that exhibit halite dissolution temperatures of 295°–495°C indicate that the circulating magmatic fluids most likely underwent significant cooling before inclusion entrapment.

The halite-bearing fluid inclusions from MARK may be explained using a model involving the simple cooling of high-salinity, magmatic fluids during the final stages of crystallization (Figs. 10, 12)(Bodnar, 1994). As shown in Figure 12, a high-salinity fluid trapped in Field A will contain a halite daughter mineral at room temperature and will homogenize by vapor bubble disappearance. Cooling of this fluid along a path such that it intersects isochore B will result in inclusions that exhibit the simultaneous disappearance of the halite daughter mineral and vapor bubble. With continued cooling, an inclusion that entraps fluid under P-T conditions represented in Field C would homogenize by halite dissolution.

Whether the brine inclusions that homogenize by halite dissolution represent magmatic fluids that were exsolved under conditions corresponding to the two-phase or to the one-phase field is not possible to unambiguously determine. In an evolving magma-hydrothermal system, rapid stress changes and thermal pulses associated with magma emplacement and spreading likely induce episodic fracture propagation in the crystalline host rocks. Pressure decreases associated with these fracturing events may promote formation of brines by supercritical phase separation, whereas more quiescent periods may be associated with brine separation in the absence of a vapor phase. Preservation of brines in the plutonic rocks from Sites 921 to 923 may reflect either of these two processes. During fluid migration along anastomosing systems of microfracture networks in the gabbroic rocks, density stratification of the brine and vapor phases (Fournier, 1988; Bischoff and Rosenbauer, 1989), coupled with preferential wetting of the fracture walls with brines (Goldfarb and Delaney, 1988), may have allowed preferential entrapment of the brines at depth as the vapors migrated to shallower crustal levels. Whatever the mechanism of brine formation was within the hydrothermal system(s) that operated at MARK, the general restriction of halite-bearing inclusions to primary apatite and quartz crystals within both the micropegmatitic patches and compositionally evolved veins indicates that late-stage magmatic fluids may be the most likely source of the 38–59 wt% NaCl equivalent salinity fluids.

Evolution of Low- to Moderate-Salinity Fluids

Low- to moderate-salinity inclusions in plutonic rocks from Sites 921 to 923 that range from ~1.0 to ~20 wt% NaCl are broadly similar in composition to fluid inclusions in crustal Layer 3 rocks from other spreading environments (Figs. 7, 9)(e.g., Hess Deep, [Kelley and

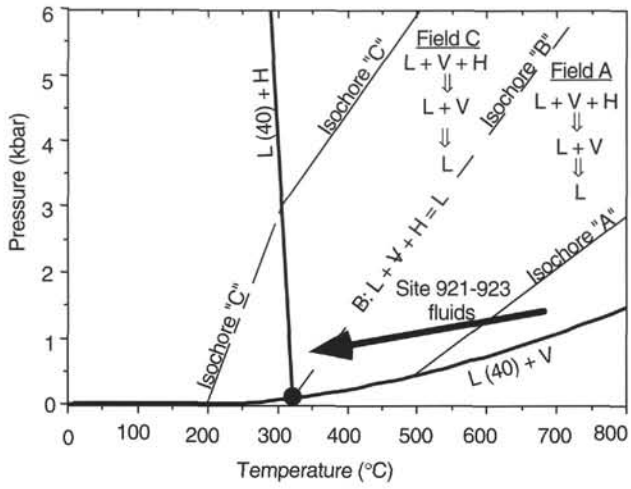

Figure 12. Schematic model for formation of brine-rich (40 wt% NaCl) inclusions that homogenize by vapor bubble disappearance, by simultaneous vapor bubble and halite disappearance, and by halite dissolution (after Bodnar, 1994). The gently sloped curve near labeled L(40) + V is the liquid + vapor curve for a solution that contains 40 wt% NaCl. The curve labeled L(40) + H is the liquidus curve.

Malpas, 1996], the MARK area of the Mid-Atlantic Ridge [Kelley et al., 1993; Delaney et al., 1987], the Troodos ophiolite, Cyprus [Kelley et al., 1992], the Mathematician Ridge [Vanko, 1988], the Oceanographer Transform Zone [Vanko et al., 1992], and the Gorringe Bank [Nehlig, 1991]). They typically exhibit equivalent fluid salinities that range from about 30% to 600% of seawater values (3.2 wt% NaCl) and exhibit uncorrected homogenization temperatures that cluster at 275°–350°C (Figs. 6, 8, 13). It is important to note, however, that these lower temperature inclusions contain some of the highest salinity fluids reported for inclusions that contain solutions unsaturated with respect to NaCl, and that the salinities are generally higher than fluids in gabbros, quartz breccias, and metabasalts previously collected from the MARK area (Fig. 13)(Kelley et al., 1993). In addition, the fluids in plutonic rocks from Sites 921 to 923 contain average salinities (6.6 wt% NaCl ± 3.7) that are almost 3 times as great as those for plutonic rocks from Hess Deep (Fig. 9)(2.7 wt% NaCl ± 3.0; Kelley and Malpas, 1996). The temperature-compositional relationships of the inclusions require a complex fluid evolution history, which may include the direct exsolution of brines from an evolved melt, the condensation of either magmatic or seawater-derived fluids, or variable mixing of hydrothermal seawater with supercritical phase-separated brines and vapors. We rule out both boiling and hydration reactions as viable processes for formation of these fluids both because the plutonic rocks were most likely formed at pressures much greater than the critical point of seawater (298 bar) and because alteration minerals that contain high concentrations of chlorine are generally rare in submarine plutonic environments.

In the absence of isotopic data on the low- to moderate-salinity fluids from MARK, it is not possible to determine whether the fluids are of a magmatic or seawater origin. In previous studies (Kelley and Delaney, 1987; Nehlig, 1991; Kelley et al., 1993; Saccocia and Gillis, 1995) compositionally similar fluids have been attributed to penetration of supercritically phase-separated hydrothermal seawater into the plutonic sequence subsequent to the collapse of the magmatic-dominated hydrothermal system; however, it may be that at Sites 921–923, generation of the low- to moderately high-salinity fluids involved a magmatic component as well. Although plagioclase-hosted fluid inclusions within the gabbroic rocks generally exhibit salinities that overlap with those of hydrothermal vent fluids and of plutonic samples from other sites (Table 2; Figs. 8, 13), in general, the most highly saline, unsaturated fluids are restricted to felsic veins that cut the gabbroic sections (Fig. 4; Table 2). This, coupled with intense alteration of the bounding host-rock associated with injection of the felsic veins, makes one consider the possibility that these fluids may be magmatic in origin. As discussed in the previous section, fluids exsolving from silicic melts under about 2 kbar pressure may evolve from initial salinities of ~20 wt% to <1 wt% NaCl as crystallization proceeds (Cline and Bodnar, 1991). The exact compositions of the fluid will depend on the initial volatile content, but in higher pressure systems the trend to lower salinity fluids with progressive fractionation should hold true for submarine systems as well.

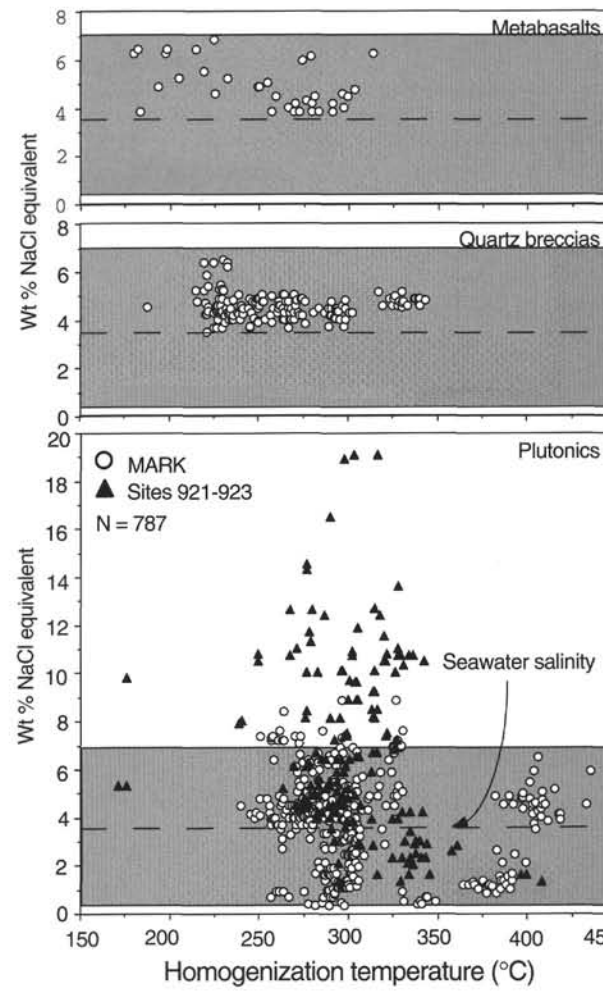

Figure 13. Uncorrected homogenization temperatures and corresponding salinities for low- to moderate-salinity inclusions hosted in gabbro, vein, quartz-breccia, and metabasalt samples recovered from the MARK area and at Sites 921–923. Previously collected plutonic-hosted inclusions exhibit a striking overlap in salinities with those measured in active hydrothermal vent fluids (stippled area). Salinities of inclusions in quartz-bearing veins from Sites 921 to 923 are enriched up to about six times that of seawater values. N denotes the number of inclusions measured.

The development of low-salinity vapors and brines by condensation, in addition to being an important process in high-temperature magmatic environments, has also been inferred to be an active process in lower-temperature, seawater-dominated systems operative beneath hydrothermal vents at 9°N on the East Pacific Rise (Von Damm et al., 1992) and on the Juan de Fuca Ridge beneath Axial Seamount and at the Endeavor segment vent field (Butterfield et al., 1990; Lilley et al., 1993; Butterfield et al., 1994). These fluids contain salinities of <1–7 wt% NaCl, similar to those of some plutonic-hosted inclusions. A seawater condensation model for the 1–20 wt% equivalent salinity fluids from Sites 921 to 923 is presented in Figure 14, which shows temperature-depth-pressure relationships in the

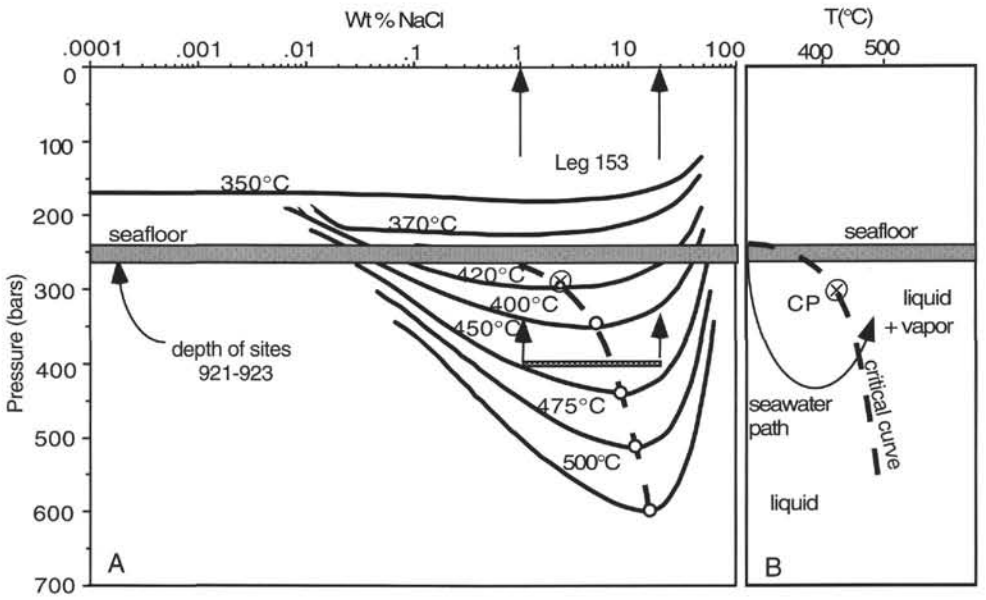

Figure 14. A seawater condensation model for the 1–20 wt% equivalent salinity fluids from Sites 921 to 923 using temperature-depth-pressure relationships in the NaCl-H_2O system under hydrostatic pressure conditions. The isotherms define a saddle-shaped field boundary that separates the one-phase liquid field from the two-phase vapor + liquid field (**A**). The position of the critical curve (dashed line), which bounds this field, is determined by the critical points of fluids ranging from H_2O to NaCl. The stippled area corresponds to the seafloor depths where drilling was initiated for Sites 921–923. Circulating seawater-like fluids that intersect the portion of the curve at conditions less than the critical point (CP = 298 bar and 407°C for seawater) will undergo boiling. At temperatures and pressures greater than the critical point, seawater-like fluids that intersect the two-phase condensation curve will separate out droplets of brine from a low-salinity vapor (arrow in **B**). Assuming that the 1 and 20 wt% NaCl equivalent fluids in Site 921–923 plutonic rocks represent end-member fluids would require formation temperatures of ~450°C and ~400 bar pressure.

NaCl-H_2O system under hydrostatic pressure conditions (after Bischoff and Rosenbauer, 1988; Bischoff, 1991). The isotherms shown define a saddle-shaped field boundary that separates the one-phase liquid field from the two-phase vapor + liquid field. The position of the critical curve (dashed line), which bounds this field, is determined by the critical points of fluids ranging from H_2O to NaCl. The stippled area corresponds to the seafloor depths where drilling was initiated for Sites 921–923. In an evolving magma-hydrothermal system, as seawater-derived fluids migrate to depth, they must traverse a series of compositionally dependent condensation curves as the heat source is approached. Circulating seawater-like fluids that intersect the portion of the curve at conditions less than the critical point (CP = 298 bar and 407°C for seawater) will undergo boiling. At temperatures and pressures greater than the critical point, seawater-like fluids that intersect the condensation portion of the curve will separate out droplets of brine from a low-salinity vapor.

If the 1 and 20 wt% NaCl equivalent fluids in the Site 921–923 plutonic rocks represent end-member compositions formed by phase separation, this would require that they formed at temperatures of approximately 450°C and 400 bar pressure. In either a magmatic or seawater model involving condensation for formation of the 1–20 wt% equivalent salinity inclusions, a maximum pressure of fluid entrapment of about 700 bar is required. At pressures greater than this, condensation will cause end-member vapors with >> 1 wt% NaCl to separate because of the strong curvature of the isotherms in the NaCl-H_2O system (Fig. 15). If compositions of the fluid inclusions reflect condensation of a magmatic aqueous phase, the fluids must have undergone significant conductive cooling. This results from the fact that an increase in the homogenization temperatures of these fluids (250°–350°C) to trapping temperatures consistent with magmatic conditions would require unreasonable pressure corrections of several kilobars. It is important to note, however, that whatever the source of these fluids is, the preservation of fluids with 1 wt% NaCl salinities requires that the vapor and brine phases maintain segregation subsequent to phase separation and that little, if any, mixing with seawater occurred. The anastomosing microfracture systems in the plutonic rocks may provide a favorable environment for such processes because in large aperture, high flow through fractures, flow is likely to be turbulent, and brine and vapor phases may not remain immiscible. In contrast, in small aperture, less continuous fracture networks such as those present in the plutonic section of MARK, flow is more likely to occur under laminar conditions, and preferential wetting of the fracture walls with brines may allow the vapor and brine to coexist as discrete phases (Goldfarb and Delaney, 1988; Fox, 1990). Intermittent release of such brine and vapor-rich pools at depth during episodic fracturing events appears to be a common process affecting the compositions of fluids venting on the seafloor where salinities change from <1 wt% NaCl to 7 wt% NaCl over the lifetime of a vent system (Von Damm et al., 1992; M.D. Lilley, pers. comm., 1995).

Low-Salinity CH_4 Fluids

The origin of the $CH_4 + H_2O \pm H_2$–bearing fluids in the plutonic rocks from Sites 921 to 923 that contain up to 11 mol% CH_4 is problematic, but they are believed to be a product of seawater alteration of the gabbroic rocks or underlying ultramafic material. Methane has rarely been identified in fluids hosted in rocks from submarine environments, but it is a ubiquitous component of submarine hydrothermal vent fluids (Lilley et al., 1983; Welhan and Craig, 1983; Welhan, 1988; Von Damm, 1990; Lilley et al., 1993) and has been detected as a trace component in inclusions in mid-ocean ridge glasses (Pineau et al., 1976; Welhan and Lupton, 1987; Welhan, 1988; Javoy and Pineau, 1991). Analyses of both occluded gases and vent fluids indicate the fluids contain CH_4 concentrations of <1 mol%, whereas those of the MARK rocks contain up to 11 times these values (Fig. 11). Carbon-isotope equilibrium temperatures of the vent fluids record temperatures of 500°–>600°C and are interpreted to reflect cooling of trapped gases before incorporation into the active hydrothermal system (Welhan, 1988; Javoy and Pineau, 1991).

Accumulating evidence suggests that the mantle may be a significant source for methane in hydrothermal systems as well. Intense CH_4 degassing has been observed along the Mid-Atlantic Ridge in

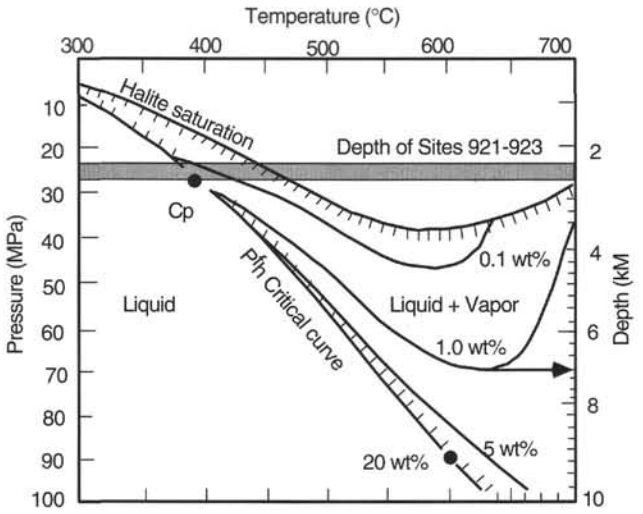

Figure 15. Isothermal (P–X) projection for the NaCl-H_2O system (after Bischoff, 1991). Isopleths (solid lines) of the solubility of NaCl in a vapor phase are shown for 0.1, 1.0, and 5.0 wt% NaCl solutions, as is the critical point for a 20 wt% NaCl solution. Also shown is the halite saturation curve and critical curve under hydrostatic conditions (P_h^f). The critical curve separates the one-phase field (Liquid) from the two-phase (Vapor + Liquid) field (bounded by hatch marks). At temperatures and pressures greater than the critical point, fluids within the two-phase field exist as droplets of brine within a vapor phase. The condensation model for generation of the ~1 wt% equivalent salinity fluids in the MARK gabbros requires that fluid circulation occurred at temperatures >407°C (the critical point of seawater) and that the inclusions were trapped at pressures less than about 70 MPa. This pressure estimate is a maximum in that, at pressures greater than 70 MPa, condensation would cause vapors with >1 wt% NaCl to separate.

crustally attenuated zones in which serpentinized peridotite bodies outcrop on the seafloor (Charlou et al., 1988; Rona et al., 1992; Charlou and Donval, 1993; Bougault et al., 1993). The close association of the plumes with serpentinized peridotite, coupled with their extremely low TDM/CH_4 ratios (total dissolved manganese/methane) is thought to reflect CH_4 production by seawater-peridotite interactions (Charlou and Donval, 1993; Bougault et al., 1993). Evidence that significant amounts of CH_4 may be generated by serpentinization processes is provided by pore-waters sampled during ODP Leg 125 at a serpentinized seamount in the Mariana forearc where high concentrations of CH_4 and C_2H_6 were measured (Haggerty, 1989; Mottl and Haggerty, 1989). CH_4 seeps have also been observed emanating from serpentinized bodies in the Zambales ophiolite in the Philippines (Abrajano et al., 1988). Data on the Zambales ophiolite suggest that fluids that have reacted with ultramafic rocks are dominated by CH_4, totally lack or contain only trace amounts of CO_2, and contain elevated concentrations of H_2. These data are consistent with experimental investigations of seawater reaction with ultramafic material at 200°–300°C, and 500 bar that show both CH_4 and H_2 as reaction by-products (Janecky and Seyfried, 1986).

Serpentinization processes in ultramafic and mafic rocks involve complex reactions that require the infiltration of large amounts of water and that are commonly accompanied at the serpentinization front by conditions of extremely low fO_2 (Frost, 1985). In these systems, the fO_2 is controlled by equilibria among oxide and silicate phases following a general reaction such as

$$12 \text{ olivine} + 12\ H_2O + O_2 = 6 \text{ serpentine} + 2 \text{ magnetite}.$$

Reduction occurs as a result of oxidation of ferrous iron (Fe^{2+}) in the silicate phases to form ferric iron (Fe^{3+}) in magnetite. Because the oxygen required for this reaction is obtained from the hydrothermal fluid, substantial amounts of both H_2 may be generated (Frost, 1985; Alt and Anderson, 1991). Reducing conditions will be maintained in this system as long as the water- to-rock ratios are low and olivine remains as a mineral phase. The composition of any carbon-bearing fluids present during migration of the reduction front will be greatly affected by the fO_2 such that, any CO_2 in the initial fluid will undergo reduction to $CH_4 \pm C$ (graphite) (Frost, 1985; Mathez et al., 1989), following a reaction similar to

$$CO_2 + 4\ H_2 = CH_4 + 2\ H_2O.$$

Abiogenic CH_4 production by high-temperature water-rock reactions has recently been documented in plutonic rocks recovered from Hole 735B on the Southwest Indian Ridge (Kelley and Früh-Green, 1995). Mineral-fluid equilibria of CH_4-$H_2O \pm H_2$ + graphite inclusions in the Southwest Indian Ridge rocks that contain up to 40 mol% CH_4 and that are similar to those from Sites 921 to 923 (Fig. 11) indicate that the inclusions were entrapped under equilibrium conditions at minimum temperatures of 400°C and at very near to QFM conditions (Kelley, 1996). Isotopic compositions of these fluids ($\delta^{13}CCH_4 = -9.1$ to -27.4‰; $\delta DCH_4 = -99$ to -149‰) do not support either a biogenic or thermogenic origin for the CH_4, but are consistent with formation involving seawater alteration of the plutonic rocks at high temperatures (Kelley and Früh-Green, 1995). That similar processes were most likely responsible for formation of the CH_4-$H_2O \pm H_2$ inclusions in plutonic rocks from Sites 921 to 923 is indicated by the fact that the fluids contain CH_4 concentrations that are >11 times those of vent or basaltic-hosted fluids, that they contain measurable quantities of H_2, and that fluid circulation probably occurred in a sediment-poor environment.

CONCLUSIONS

The thermal and compositional evolution of fluids in crustal Layer 3 rocks from Sites 921 to 923 at the MARK area reflect a complicated history involving multiple magma-hydrothermal pulses as the rocks cooled and were transported away from the zone of crustal accretion. Early fluids to be exsolved from the basaltic melts involved CO_2-rich vapors, which with progressive fractionation evolved to more H_2O-rich compositions. These later fluids were most likely exsolved under immiscible conditions and involved the development of CO_2-H_2O-rich vapors and CO_2-H_2O-NaCl brines that were trapped during mineral growth, as well as during later high-temperature fracturing events. Subsequent cooling of the high-salinity, magmatic fluids during the final stages of crystallization, or direct exsolution of brines from the late-stage melts, resulted in formation of fluids with salinities of 38–59 wt% NaCl that were trapped in pegmatitic pods, and trondhjemitic to dioritic veins that cut the plutonic sequence. The transition from magmatic-to hydrothermal seawater-dominated conditions in the plutonic rocks may be represented by penetration of fluids that contain salinities that range from near seawater, to six times seawater values (1–20 wt% NaCl equivalent) at temperatures of ~275°–350°C. The healed flow channels are most commonly marked by an irregular microscopic network of actinolitic veins, which rim grain boundaries and overprint high-temperature deformation fabrics. Migration of these fluids along microfracture and vein networks resulted in the heterogeneous replacement of the gabbroic rocks by greenschist facies to transitional amphibolite mineral assemblages. This alteration is most intense adjacent to vein networks and in cataclastically deformed zones in which brittle failure facilitated enhanced fluid flow.

In localized zones throughout the cores, circulating CH_4-H_2O-rich fluids contain CH_4 concentrations that are 11 times those of both submarine hydrothermal vent fluids and of basaltic-hosted gases. The high concentration of $CH_4 \pm H_2$ in these fluids (~11 mol%) is believed to reflect seawater penetration and associated serpentinization at tem-

peratures of 400°C with mafic minerals within the gabbroic rocks or with ultramafic material that underlie the plutonic sequence. The presence of CH_4-rich fluids in plutonic rocks from Sites 921 to 923 and from adjacent areas in the MARK area, their ubiquitous occurrence throughout plutonic samples from Hole 735B at the Southwest Indian Ridge, and the discovery of intense CH_4 anomalies associated with ultramafic outcrops along the Mid-Atlantic Ridge indicate that these fluids may be a significant and previously unrecognized source for these volatile species, particularly in hydrothermal systems associated with slow-spreading environments where faulting allows enhanced penetration of fluids into crustal Layer 3 and upper mantle rocks.

ACKNOWLEDGMENTS

This paper benefited from the helpful reviews by P. Saccocia and J. Peters. Special thanks is given to J. Frantz for analyses of the inclusions using micro-Raman spectroscopy at the Geophysical Laboratory, Carnegie Institution of Washington, Washington, D.C. This research was funded by a grant from JOI/USSAC through the Texas A&M Research Foundation. Contribution 2154, School of Oceanography, University of Washington.

REFERENCES

Abrajano, T.A., Sturchio, N.C., Bohlke, J.K., Lyon, G.L., Poreda, R.J., and Stevens, C.M., 1988. Methane-hydrogen gas seeps, Zambales Ophiolite, Philippines: deep or shallow origin? *Chem. Geol.,* 71:211–222.

Alt, J.C., and Anderson, T.F., 1991. Mineralogy and isotopic composition of sulfur in layer 3 gabbros from the Indian Ocean, Hole 735B. *In* Von Herzen, R.P., Robinson, P.T., et al., *Proc. ODP, Sci. Results,* 118: College Station, TX (Ocean Drilling Program), 113–126.

Baker, E.T., Massoth, G.J., Feely, R.A., Embley, R.W., Thomson, R.E., and Burd, B.J., 1995. Hydrothermal event plumes from the CoAxial seafloor eruption site, Juan de Fuca Ridge. *Geophys. Res. Lett.,* 22:147–150.

Baker, E.T., Massoth, G.J., Walker, S.L., and Embley, R.W., 1993. A method for quantitatively estimating diffuse and discrete hydrothermal discharge. *Earth Planet. Sci. Lett.,* 118:235–249.

Bischoff, J.L., 1991. Densities of liquids and vapors in boiling NaCl-H_2O solutions: a PTVX summary from 300° to 500°C. *Am. J. Sci.,* 291:309–338.

Bischoff, J.L., and Rosenbauer, R.J., 1988. Liquid-vapor relations in the critical region of the system NaCl-H_2O from 380°C to 415°C: a refined determination of the critical point and two-phase boundary of seawater. *Geochim. Cosmochim. Acta,* 52:2121–2126.

Bischoff, J.L., and Rosenbauer, R.J., 1989. Salinity variation in submarine hydrothermal systems by layered double-diffusive convection. *J. Geol.,* 97:613–623.

Bodnar, R.J., 1994. Synthetic fluid inclusions: XII. The system H_2O-NaCl. Experimental determination of the halite liquidus and isochores for a 40 wt% NaCl solution. *Geochim. Cosmochim. Acta,* 58:1053–1063.

Bougault, H., Charlou, J.L., Fouquet, Y., Needham, H.D., Vaslet, N., Appriou, P., Baptiste, P.J., Rona, P.A., Dmitriev, L., and Silantiev, S., 1993. Fast and slow spreading ridges: structure and hydrothermal activity, ultramafic topographic highs, and CH_4 output. *J. Geophys. Res.,* 98:9643–9651.

Brown, J.R., and Karson, J.A., 1988. Variations in axial processes on the Mid-Atlantic Ridge: the median valley of the MARK area. *Mar. Geophys. Res.,* 10:109–138.

Burnham, C.W., 1979. Magma and hydrothermal fluids. *In* Barnes, H.L. (Ed.), *Geochemistry of Hydrothermal Ore Deposits:* New York (Wiley), 71–133.

Butterfield, D.A., Massoth, G.J., McDuff, R.E., Lupton, J.E., and Lilley, M.D., 1990. Geochemistry of hydrothermal fluids from Axial Seamount Hydrothermal Emissions Study vent field, Juan de Fuca Ridge: subseafloor boiling and subsequent fluid-rock interaction. *J. Geophys. Res.,* 95:12895–12921.

Butterfield, D.A., McDuff, R.E., Mottl, M.J., Lilley, M.D., Lupton, J.E., and Massoth, G.J., 1994. Gradients in the composition of hydrothermal fluids from the Endeavour segment vent field: phase separation and brine loss. *J. Geophys. Res.,* 99:9561–9583.

Cannat, M., Juteau, T., and Berger, E., 1990. Petrostructural analysis of the Leg 109 serpentinized peridotites. *In* Detrick, R., Honnorez, J., Bryan, W.B., Juteau, T., et al., *Proc. ODP, Sci. Results,* 106/109: College Station, TX (Ocean Drilling Program), 47–57.

Charlou, J.L., Bougault, H., Appriou, P., Nelsen, T., and Rona, P., 1992. Different TDM/CH_4 hydrothermal plume signatures: TAG site at 26°N and serpentinized ultrabasic diapir at 15°05′N on the Mid-Atlantic Ridge. *Geochim. Cosmochim. Acta,* 55:3209–3222.

Charlou, J.L., Dmitried, L., Bougault, H., and Needham, H.D., 1988. Hydrothermal CH_4 between 12°N and 15°N over the Mid-Atlantic Ridge. *Deep-Sea Res.,* 35:121–131.

Charlou, J.-L., and Donval, J.-P., 1993. Hydrothermal methane venting between 12°N and 26°N along the mid-Atlantic ridge. *J. Geophys. Res.,* 98:9625–9642.

Cline, J.S., and Bodnar, R.J., 1991. Can economic porphyry copper mineralization be generated by a typical calc-alkaline melt? *J. Geophys. Res.,* 96:8113–8126.

Cormier, M.-H., Detrick, R.S., and Purdy, G.M., 1984. Anomalously thin crust in oceanic fracture zones: new seismic constraints from the Kane Fracture Zone. *J. Geophys. Res.,* 89:10249–10266.

Delaney, J.R., Baross, J.A., Lilley, M.D., and Kelley, D.S., 1994. Is the quantum event of crustal accretion: a window into the deep-hot biosphere. *Eos (Fall meeting suppl.),* 75:617.

Delaney, J.R., Mogk, D.W., and Mottl, M.J., 1987. Quartz-cemented breccias from the Mid-Atlantic Ridge: samples of a high-salinity hydrothermal upflow zone. *J. Geophys. Res.,* 92:9175–9192.

Delaney, J.R., Muenow, D.W., and Graham, D.G., 1978. Abundance and distribution of water, carbon, and sulfur in the glassy rims of submarine pillow basalts. *Geochim. Cosmochim. Acta,* 42:581–594.

Demming, J.W., and Baross, J.A., 1993. Deep-sea smokers: windows to a subsurface biosphere. *Geochim. Cosmochim. Acta,* 57:3219–3230.

Detrick, R.S., Fox, P.J., Kastens, K., Bryan, W.B.F., Mayer, L., Karson, J., and Pockalny, R.A., 1984. Seabeam survey of the Kane Fracture Zone and adjacent Mid-Atlantic ridge rift valley. *Eos,* 65:1006.

Dixon, J.E., Stolper, E., and Delaney, J.R., 1988. Infrared spectroscopic measurements of CO_2 and H_2O in Juan de Fuca Ridge basaltic glasses. *Earth Planet. Sci. Lett.,* 90:87–104.

Embley, R.W., Chadwick, W.W., Jonasson, I.R., Butterfield, D.A., and Baker, E.T., 1995. Initial results of the rapid response to the 1993 CoAxial event: relationship between hydrothermal and volcanic processes. *Geophys. Res. Lett.,* 22:143–146.

Fine, G., and Stolper, E., 1986. Dissolved carbon dioxide in basaltic glasses: concentrations and speciation. *Earth Planet. Sci. Lett.,* 76:263–278.

Fournier, R.O., 1987. Conceptual models of brine evolution in magmatic-hydrothermal systems. *Geol. Surv. Prof. Pap. U.S.,* 1350:1487–1506.

Fox, C., 1990. Consequences of phase separation on the distribution of hydrothermal fluids at ASHES vent field, Axial Volcano, Juan de Fuca Ridge. *J. Geophys. Res.,* 95:12923–12926.

Frantz, J.D., Popp, R.K., and Hoering, T.C., 1992. The compositional limits of fluid immiscibility in the system H_2O-NaCl-CO_2 as determined with the use of synthetic fluid inclusions in conjunction with mass spectrometry. *Chem. Geol.,* 98:237–256.

Frost, B.R., 1985. On the stability of sulfides, oxides, and native metals in serpentine. *J. Petrol.,* 26:31–63.

Gallinatti, B.C, 1984. Initiation and collapse of active circulation in a hydrothermal system at the Mid-Atlantic Ridge, 23°N. *J. Geophys. Res.,* 89:3275–3289.

Gente, P., Mével, C., Auzende, J.-M., Karson, J.A., and Fouquet, Y., 1991. An example of a recent accretion on the Mid-Atlantic Ridge: the Snake Pit neovolcanic ridge (MARK area: 23°22′N). *Tectonophysics,* 190:1–29.

Gillis, K.M., 1996. Rare earth element constraints on the origin of amphibole in gabbroic rocks from Site 894, Hess Deep. *In* Mével, C., Gillis, K.M., Allan, J.F., and Meyer, P.S. (Eds.), *Proc. ODP, Sci. Results,* 147: College Station, TX (Ocean Drilling Program), 59–75.

Gillis, K.M., Thompson, G., and Kelley, D.S., 1993. A view of the lower crustal component of hydrothermal systems at the Mid-Atlantic Ridge. *J. Geophys. Res.,* 98:19597–19619.

Goldfarb, M.S., and Delaney, J.R., 1988. Response of two-phase fluids to fracture configurations within submarine hydrothermal systems. *J. Geophys. Res.,* 93:4585–4594.

Haggerty, J.A., 1989. Fluid inclusion studies of chimneys associated with serpentinite seamounts in the Mariana forearc. *Proc. 2nd Pan-Am. Res. Fluid Incs,* 29.

Haymon, R.M., Fornari, D.J., Von Damm, K.L., Lilley, M.D., Perfit, M.R., Edmond, J.M., Shanks, W.C., III, Lutz, R.A., Grebmeier, J.M., Carbotte, S., Wright, D., McLaughlin, E., Smith, M., Beedle, N., and Olson, E., 1993. Volcanic eruption of the mid-ocean ridge along the East Pacific Rise crest at 9°45–52′N: direct submersible observations of seafloor phenomena associated with an eruption event in April, 1991. *Earth Planet. Sci. Lett.,* 119:85–101.

Herzberg, G., 1951. Molecular spectra and molecular structure. In *Infrared and Raman Spectra:* New York (Van Nostrand Reinhold).

Janecky, D.R., and Seyfried, W.E., Jr., 1986. Hydrothermal serpentinization of peridotite within the oceanic crust: experimental investigations of mineralogy and major element chemistry. *Geochim. Cosmochim. Acta,* 50:1357–1378.

Javoy, M., and Pineau, F., 1991. The volatiles record of a "popping" rock from the Mid-Atlantic Ridge at 14°N: chemical and isotopic composition of gas trapped in the vesicles. *Earth Planet. Sci. Lett.,* 107:598–611.

Jean-Baptiste, P., Charlou, J.L., Stievenard, M., Donval, J.P., Bougault, H., and Mével, C., 1991. Helium and methane measurements in hydrothermal fluids from the Mid-Atlantic Ridge: The Snake Pit site at 23°N. *Earth Planet. Sci. Lett.,* 106:17–28.

Karson, J.A., 1990. Seafloor spreading on the Mid-Atlantic Ridge: implications for the structure of ophiolites and oceanic lithosphere produced in slow-spreading environments. *In* Malpas, J., Moores, E.M., Panayiotou, A., and Xenophontos, C. (Eds.), *Ophiolites: Oceanic Crustal Analogues:* Proc. Symp. "Troodos 1987": Nicosia, Cyprus (Minist. Agric. Nat. Resour.), 547–555.

Karson, J.A., and Dick, H.J.B., 1983. Tectonics of ridge-transform intersections at the Kane Fracture Zone. *Mar. Geophys. Res.,* 6:51–98.

Karson, J.A., Thompson, G., Humphris, S.E., Edmond, J.M., Bryan, W.B., Brown, J.R., Winters, A.T., Pockalny, R.A., Casey, J.F., Campbell, A.C., Klinkhammer, G., Palmer, M.R., Kinzler, R.J., and Sulanowska, M.M., 1987. Along-axis variations in seafloor spreading in the MARK area. *Nature,* 328:681–685.

Kelley, D.S., 1996. Methane-rich fluids in the oceanic crust. *J. Geophys. Res.,* 101:2943–2962.

Kelley, D.S., and Delaney, J.R., 1987. Two-phase separation and fracturing in mid-ocean ridge gabbros at temperatures greater than 700°C. *Earth Planet. Sci. Lett.,* 83:53–66.

Kelley, D.S., and Früh-Green, G.L., 1995. Methane concentrations and isotopic compositions in layer 3 of the oceanic crust. *Eos,* 76:44.

Kelley, D.S., Gillis, K.M., and Thompson, G., 1993. Fluid evolution in submarine magma-hydrothermal systems at the Mid-Atlantic Ridge. *J. Geophys. Res.,* 98:19579–19596.

Kelley, D.S., Hoering, T., and Frantz, J.D., 1994. Methane-rich fluids in gabbroic rocks from the Southwest Indian Ridge: results from mass spectrometric analyses. *Eos,* 44:657.

Kelley, D.S., and Malpas, J., 1996. Melt-fluid evolution in gabbroic rocks from Hess Deep. *In* Mével, C., Gillis, K.M., Allan, J.F., and Meyer, P.S. (Eds.), *Proc. ODP, Sci. Results,* 147: College Station, TX (Ocean Drilling Program), 213–226.

Kelley, D.S., Robinson, P.T., and Malpas, J.G., 1992. Processes of brine generation and circulation in the oceanic crust: fluid inclusion evidence from the Troodos ophiolite, Cyprus. *J. Geophys. Res.,* 97:9307–9322.

Kong, L.S.L., Detrick, R.S., Fox, P.J., Mayer, L.A., and Ryan, W.F.B., 1989. The morphology and tectonics of the MARK area from Sea Beam and MARC 1 observations (Mid-Atlantic Ridge 23°N). *Mar. Geophys. Res.,* 10:59–90.

Lilley, M.D., 1994. The behavior of CO_2, H_2, and CH_4 in nascent hydrothermal systems. *Eos (Fall Meet. Suppl.),* 75:618.

Lilley, M.D., Baross, J.A., and Gordon, L.I., 1983. Reduced gases and bacteria in hydrothermal fluids: the Galapagos spreading center and 21°N East Pacific Rise. *In* Rona, P.A., Bostrom, K., Laubier, L., and Smith, K.L., Jr. (Eds.), *Hydrothermal Processes at Seafloor Spreading Centers:* New York (Plenum), 411–447.

Lilley, M.D., Butterfield, D.E., Olson, E.J., Lupton, J.E., Mackos, S.A., and McDuff, R.E., 1993. Anomalous CH_4 and NH_4 concentrations at an unsedimented mid-ocean ridge hydrothermal system. *Nature,* 364:45–47.

Lilley, M.D., Lupton, J.E., and Von Damm, K.L. 1992. Volatiles in the 9°N hydrothermal system: a comparison of 1991 and 1992 data. *Eos (Fall Meet. Suppl.),* 73:524.

Liou, J.G., Kuniyoshi, S., and Ito, K., 1974. Experimental studies of the phase relations between greenschist and amphibolite in a basaltic system. *Am. J. Sci.,* 274:613–632.

Lupton, J.E., 1983. Terrestrial inert gases: isotope tracer studies and clues to primordial components in the mantle. *Annu. Rev. Earth Planet. Sci.,* 11:371–414.

Lupton, J.E., Baker, E.T., and Massoth, G.J., 1989. Variable ^3He/heat ratios in submarine hydrothermal systems: evidence from two plumes over the Juan de Fuca Ridge. *Nature,* 337:161–163.

Lupton, J.E., and Craig, H., 1981. A major helium-3 source at 15°S on the East Pacific Rise. *Science,* 214:13–18.

Mathez, E.A., Dietrich, V.J., Holloway, J.R., and Boudreau, A.E., 1989. Carbon distribution in the Stillwater Complex and evolution of vapor during crystallization of Stillwater and Bushveld magmas. *J. Petrol.,* 30:153–173.

Mével, C., Cannat, M., Gente, P., Marion, E., Auzende, J.-M., and Karson, J.A., 1991. Emplacement of deep crustal and mantle rocks on the west median valley wall of the MARK area (MAR 23°N). *Tectonophysics,* 190:31–53.

Moore, J.G., 1977. Water content of basalt erupted on the ocean floor. *Contrib. Mineral. Petrol.,* 28:272–279.

Mottl, M.J., and Haggerty, J.A., 1989. Upwelling of Cl-poor, S and C-rich waters through a serpentinite seamount, Mariana Forearc, ODP Leg 125. *Eos,* 70:1382.

Nehlig, P., 1991. Salinity of oceanic hydrothermal fluids: a fluid inclusion study. *Earth Planet. Sci. Lett.,* 102:310–325.

Pawley, A.R., Holloway, J.R., and McMillan, P.F., 1992. The effect of oxygen fugacity on the solubility of carbon-oxygen fluids in basaltic melt. *Earth Planet. Sci. Lett.,* 110:213–225.

Pedersen, R.B., 1986. The nature and significance of magma chamber margins in ophiolites: examples from the Norwegian Caledonides. *Earth Planet. Sci. Lett.,* 77:100–112.

Pedersen, R.B., and Malpas, J., 1984. The origin of oceanic plagiogranites from the Karmoy ophiolite, western Norway. *Contrib. Mineral. Petrol.,* 88:36–52.

Pineau, F., Javoy, M., and Bottinga, Y., 1976. $^{13}C/^{12}C$ ratios of rocks and inclusions in popping rocks of the Mid-Atlantic Ridge. *Earth Planet. Sci. Lett.,* 29:413–421.

Pockalny, R.A., Detrick, R.S., and Fox, P.J., 1988. Morphology and tectonics of the Kane Transform from Sea Beam bathymetry data. *J. Geophys. Res.,* 93:3179–3193.

Purdy, G.M., and Detrick, R.S., 1986. Crustal structure of the Mid-Atlantic Ridge at 23°N from seismic refraction studies. *J. Geophys. Res.,* 91:3739–3762.

Roedder, E., 1984. Fluid inclusions. *Rev. Mineral., Mineral. Soc. Am.,* 12.

Rona, P., Bougault, H., Charlou, J.L., Appriou, P., Nelsen, T., Tefry, T.H., Eberhart, G.L., Barone, A., and Needham, H.D., 1992. Hydrothermal circulation, serpentinization, and degassing at a rift valley-fracture zone intersection: Mid-Atlantic Ridge near 15°N, 45°W. *Geology,* 20:783–786.

Saccocia, P.J., and Gillis., K.M., 1995. Hydrothermal upflow zones in the oceanic crust. *Earth Planet. Sci. Lett.,* 136:1–16.

Schrotter, H.W., and Klockner, H.W., 1979. Raman scattering cross sections in gases and liquids. *In* Weber, A. (Ed.), *Raman Spectroscopy of Gases and Liquids:* Berlin (Springer-Verlag), 3:123–166.

Schulz, N.J., Detrick, R.S., and Miller, S.P., 1988. Two- and three-dimensional inversions of magnetic anomalies in the MARK area (Mid-Atlantic Ridge, 23°N). *Mar. Geophys. Res.,* 10:41–57.

Seitz, J.C., and Pasteris, J.D., 1990. Theoretical and practical aspects of differential partitioning of gases by clathrate hydrates in fluid inclusions. *Geochim. Cosmochim. Acta.,* 54:631–639.

Shipboard Scientific Party, 1995. Site 920. *In* Cannat, M., Karson, J.A., Miller, D.J., et al., *Proc. ODP, Init. Repts.,* 153: College Station, TX (Ocean Drilling Program), 45–119.

Simoneit, B.R., 1993. Aqueous high-temperature and high pressure organic geochemistry of hydrothermal vent systems. *Geochim. Cosmochim. Acta,* 57:3231–3243.

Sparks, R.S.J., Barclay, J., Jaupart, C., Mader, H.M., and Phillips, J.C., 1994. Physical aspects of magma degassing. I. Experimental and theoretical constraints on vesiculation. *In* Carroll, M.R., Holloway, J.R., and Ribbe, P.H. (Eds.), *Volatiles in Magma.* Rev. Mineral., 30:413–445.

Spear, F.S., 1981. An experimental study of hornblende stability and compositional variability in amphibolite. *Am. J. Sci.,* 281:697–734.

Stakes, D., Mével, C., Cannat, M., and Chaput, T., 1991. Metamorphic stratigraphy of Hole 735B. *In* Von Herzen, R.P., Robinson, P.T., et al., *Proc. ODP, Sci. Results,* 118: College Station, TX (Ocean Drilling Program), 153–180.

Stakes, D.S., 1991. Oxygen and hydrogen isotope compositions of oceanic plutonic rocks: high-temperature deformation and metamorphism of oceanic layer 3. *In* Taylor, H.P., Jr., O'Neil, J.R., and Kaplan, I.R. (Eds.), *Stable Isotope Geochemistry: A Tribute to Samuel Epstein.* Spec. Publ. Geochem. Soc., 3:77–90.

Stolper, E., and Holloway, J.R., 1988. Experimental determination of the solubility of carbon dioxide in molten basalt at low pressure. *Earth Planet. Sci. Lett.,* 87:397–408.

Taylor, W.R., and Green, D.H., 1987. The petrogenetic role of methane: effect on liquidus phase relations and the solubility mechanism of reduced C-H volatiles, *In* Mysen, B.O. (Ed.), *Magmatic Processes: Physicochemical Principles.* Geochem. Soc., Spec. Publ.,1:121–138.

Vanko, D.A., 1988. Temperature, pressure, and composition of hydrothermal fluids with their bearing on the magnitude of tectonic uplift at mid-ocean ridges, inferred from fluid inclusions in oceanic layer 3 rocks. *J. Geophys. Res.,* 93:4595–4611.

Vanko, D.A., Griffith, J.D., and Erickson, C.L., 1992. Calcium-rich brines and other hydrothermal fluids in fluid inclusions from plutonic rocks, Oceanographer Transform, Mid-Atlantic Ridge. *Geochim. Cosmochim. Acta,* 56:35–47.

Vanko, D.A., and Stakes, D.S., 1991. Fluids in oceanic layer 3: evidence from veined rocks, Hole 735B, Southwest Indian Ridge. *In* Von Herzen, R.P., Robinson, P.T., et al., *Proc. ODP, Sci. Results,* 118: College Station, TX (Ocean Drilling Program), 181–215.

Von Damm, K.L., 1990. Seafloor hydrothermal activity: black smoker chemistry and chimneys. *Annu. Rev. Earth Planet. Sci.,* 18:173–204.

Von Damm, K.L., Colodner, D.C., and Edmonds, H.N., 1992. Hydrothermal fluid chemistry at 9–10°N EPR: big changes and still changing. *Eos,* 73:524.

Welhan, J.A., 1988. Origins of methane in hydrothermal systems. *Chem. Geol.,* 71:183–198.

Welhan, J.A., and Craig, H., 1983. Methane, hydrogen and helium in hydrothermal fluids. *In* Rona, P.A., Bostrom, K., Laubier, L., and Smith, A.K.L., Jr. (Eds.), *Hydrothermal Processes at Sea Floor Spreading Centers:* New York (Plenum), 391–409.

Welhan, J.A., and Lupton, J.E., 1987. Light hydrocarbon gases in Guaymas Basin hydrothermal fluids: thermogenic versus abiogenic origin. *AAPG Bull.,* 71:215–223.

Wyllie, P.J., 1977. Crustal anatexis: an experimental review. *Tectonophysics,* 43:41–71.

Zhang, Y., and Frantz, J.D., 1987. Determination of the homogenization temperatures and densities of supercritical fluids in the system NaCl-KCl-$CaCl_2$-H_2O using synthetic fluid inclusions. *Chem. Geol.,* 64:335–350.

————, 1992. Hydrothermal reaction involving equilibrium between minerals and mixed volatiles. II. Investigations of fluid properties in the CO_2-CH_4-H_2O system using synthetic fluid inclusions. *Chem. Geol.,* 100:51–72.

Date of initial receipt: 1 August 1995
Date of acceptance: 26 January 1996
Ms 153SR-038